Development 140, 3777-3786 (2013) doi:10.1242/dev.093948

Notch signaling represses p63 expression in the developing surface ectoderm

Ana Mafalda Baptista Tadeu and Valerie Horsley*

SUMMARY

The development of the mature epidermis requires a coordinated sequence of signaling events and transcriptional changes to specify surface ectodermal progenitor cells to the keratinocyte lineage. The initial events that specify epidermal keratinocytes from ectodermal progenitor cells are not well understood. Here, we use both developing mouse embryos and human embryonic stem cells (hESCs) to explore the mechanisms that direct keratinocyte fate from ectodermal progenitor cells. We show that both hESCs and murine embryos express p63 before keratin 14. Furthermore, we find that Notch signaling is activated before p63 expression in ectodermal progenitor cells. Inhibition of Notch signaling pharmacologically or genetically reveals a negative regulatory role for Notch signaling in p63 expression during ectodermal specification in hESCs or mouse embryos, respectively. Taken together, these data reveal a role for Notch signaling in the molecular control of ectodermal progenitor cell specification to the epidermal keratinocyte lineage.

KEY WORDS: Keratinocyte specification, Notch signaling, Ectoderm, p63

INTRODUCTION

During development, the epidermis derives from the primitive ectoderm, a single layer of epithelial cells that will differentiate into epidermal keratinocytes, stratify and form the mature epithelium of the skin. In the mouse embryo, the cells of primitive ectoderm express keratin 8 (K8; Krt8 – Mouse Genome Informatics) and K18 and generate the periderm, an outer layer of epithelial cells that expresses K6 and K17 (McGowan and Coulombe, 1998; Sanes et al., 1986). Beginning at approximately embryonic day (E) 8.5, some surface ectoderm cells activate expression of K5 and K14, an indication of a commitment to the epidermal keratinocyte fate (Byrne et al., 1994; Fuchs, 2007; Koster and Roop, 2007; Nagarajan et al., 2008). After the formation of this epidermal basal layer, asymmetric divisions (Lechler and Fuchs, 2005) form suprabasal layers populated by terminally differentiated epidermal cells. Around E18.5 the epidermis reaches full maturation, producing an intact barrier (Candi et al., 2005). Although several studies have identified the molecular mechanisms that regulate epidermal formation following stratification (Blanpain and Fuchs, 2006), what controls the initial commitment of surface ectoderm to the epidermal lineage during embryogenesis is largely unknown.

The p53 homolog p63 is one of the earliest transcription factors expressed during epidermal specification (Koster and Roop, 2007) and is associated with ectodermal appendage specification, epidermal cell proliferation and development (Koster, 2010; Laurikkala et al., 2006; Lechler and Fuchs, 2005; Mills et al., 1999; Truong and Khavari, 2007; Yang et al., 1999). Alternative splicing of the *p63* gene yields transcripts encoding two classes of p63 protein isoforms, TAp63 and ΔNp63. ΔNp63 isoforms lacking the TA domain (Crum and McKeon, 2010; King and Weinberg, 2007) are highly expressed in the early stages of epidermal development and are maintained within the basal layer of the skin (Koster and Roop, 2004; Laurikkala et al., 2006; Romano et al., 2007; Romano et al., 2009). Complete ablation of all *p63* isoforms during mouse development leads to limb truncations, craniofacial malformations and the lack of an intact and functional epidermis (Mills et al., 1999; Yang et al., 1999). However, whether p63 controls epithelial progenitor self-renewal and/or lineage commitment to an epidermal fate remains controversial (Koster and Roop, 2004; Mills et al., 1999; Romano et al., 2012; Yang et al., 1999).

Notch signaling has been implicated in controlling epithelial development in a number of tissues (Blanpain et al., 2006; Bouras et al., 2008). Activation of Notch signaling involves the juxtaposition of Notch receptors and ligands on neighboring cells and activation of proteolytic cleavage of the intracellular domain of the Notch receptor (NICD) by the ADAM and γ-secretase complex. NICD translocates to the nucleus, where it interacts with the DNA-binding protein CSL/RBP-Jk and the coactivator Mastermind to promote the transcription of Notch target genes (Kopan and Ilagan, 2009). In the skin, canonical Notch signaling is required for the commitment of basal keratinocytes to terminal differentiation during development (Blanpain et al., 2006; Moriyama et al., 2008; Nguyen et al., 2006; Pan et al., 2004). However, whether Notch signaling regulates epidermal keratinocyte specification directly is not known.

In this study, we used both embryonic mouse skin and human embryonic stem cells (hESCs) to probe the mechanisms that regulate the transition from ectoderm to keratinocyte fate. We identified a previously unappreciated step of keratinocyte specification involving the expression of p63 in ectodermal progenitor cells. We found that Notch signaling is transiently active in ectodermal cells before p63 or K14 expression. By inhibiting Notch signaling pharmacologically in hESCs or genetically in mouse embryos, we found that repression of Notch signaling promotes p63 expression in ectodermal cells. Together, these results reveal a novel molecular step controlling surface ectoderm specification during the development of mammalian epidermis.

MATERIALS AND METHODS

Mice

K14-H2BGFP transgenic mice (Tumbar et al., 2004) and *PS1*$^{-/-}$;*PS2*$^{-/-}$ knockout mice (Pan et al., 2004; Saura et al., 2004) were described

Department of Molecular, Cell and Developmental Biology, Yale University, 219 Prospect Street, Box 208103, New Haven, CT 06520, USA.

*Author for correspondence (valerie.horsley@yale.edu)

Accepted 24 June 2013

previously. *PS1*$^{-/-}$*;PS2*$^{-/-}$ knockout mice were a generous gift from Raphael Kopan's laboratory at Washington University. All animals were handled according to the institutional guidelines of Yale University and Washington University.

Fluorescence-activated cell sorting and analysis

Embryos from *K14-H2BGFP* or wild-type littermates were minced and incubated in trypsin-EDTA (0.25%; Gibco) for 7 minutes at 37°C. Single cell suspensions were resuspended in fluorescence-activated cell sorting (FACS) staining buffer (4% fetal bovine serum in PBS) and stained with antibodies for E-cadherin (M108, rat, 1:400, Takara) and α6 integrin-PE (555736, rat, 1:500, BD Pharmingen). Cells were stained with the appropriate fluorophore conjugated secondary antibody and with propidium iodide (1:2000, Sigma) and sorted using FACSAria Flow Cytometer equipped with FACSDiva software (BD Biosciences). Cells were gated for single events and viability and sorted according to E-cadherin, α6 integrin and green fluorescent protein (GFP) expression. Sorted cells were collected for RNA isolation or cytospun onto glass slides at 500 rpm for 5 minutes and processed for immunofluorescence (see below).

Undifferentiated and differentiated hESCs were detached from culture plates using Trypsin-EDTA (0.05%; Stem Cell Technologies). Sample preparation was performed according to previously described protocols (Metallo et al., 2008). Briefly, cells were fixed in 1% paraformaldehyde for 10 minutes followed by permeabilization with 90% methanol. Primary antibodies for mouse keratin 14 (NCL-LL002, mouse, 1:100, Novocastra/Leica Microsystems) and keratin 18 (MAB3234, mouse, 1:300, Millipore) were incubated overnight in PBS supplemented with 2% FBS. After a 1-hour incubation in secondary antibodies, cells were analyzed on a FACSAria Flow Cytometer equipped with FACSDiva software (BD Biosciences).

hESC culture

H1 hESCs were cultured on Matrigel (BD Biosciences) in mTESR1 medium (Stem Cell Technologies) at 37°C, 5% O_2 and 5% CO_2 and passaged every 5-6 days using dispase (Stem Cell Technologies). Keratinocyte differentiation was performed according to previously described protocols (Aberdam et al., 2008). Briefly, hESC colonies were incubated for 3 days with 0.5 nM of human recombinant bone morphogenetic protein 4 (BMP4) (R&D Systems). From day 4 to day 10, BMP4 was removed and cells were incubated in medium supplemented with 10% fetal calf serum (FCII; Hyclone). To abrogate Notch signaling, the γ-secretase complex was inhibited with 5 μM DAPT (Sigma) in ethanol and replaced daily at indicated time points. Human embryonic stem cell-derived ectodermal cells were cultured on collagen-coated plates in defined keratinocyte-SFM medium (Invitrogen/Gibco). Neural differentiation was performed according to previously described protocols (Chambers et al., 2009). Briefly, cells were plated as single cells and incubated for 3 days in DMEM/F12 (Gibco), 20% Knockout Serum Replacement (Invitrogen), 0.1 mM β-ME (Sigma), 10 μM SB431542 (Tocris) and 500 ng/ml Noggin (R&D Systems). To differentiate hESCs to endoderm lineages, we followed previously described protocols (D'Amour et al., 2005). Briefly, hESC colonies were incubated for 3 days in endoderm differentiation media A containing DMEM/F12, 2 mM (1×) L-glutamine (Invitrogen) and 100 ng/ml Activin A (R&D). At day 4, growth media was replaced by endoderm differentiation media B containing DMEM/F12, 2 mM (1×) L-glutamine, 0.2% defined FBS (Hyclone) and 100 ng/ml Activin A. Finally, from day 5 to 7, colonies were incubated with endoderm differentiation media C containing DMEM/F12, 2 mM (1×) L-glutamine and 2% defined FBS. Mesoderm/trophectoderm differentiation was induced by incubating hESC colonies with 0.5 nM BMP4 for 3 days.

Western blot analysis

Cellular protein was harvested using PARP buffer (8 M urea, 2 mM EDTA, 1% SDS, 50 mM Tris-HCl pH 6.8) and quantified using a BCA protein assay (Thermo Scientific). Equal amounts of protein were resolved on an 8% polyacrylamide gel and transferred to PVDF membranes (Immobilon-P, Millipore). The membranes were blocked for 1 hour at room temperature in 5% milk in PBS supplemented with 0.1% Tween 20. After blocking, the membranes were incubated overnight with a cleaved Notch antibody-Val1744 (2421, rabbit, 1:1000, Cell Signaling) followed by incubation with an appropriate secondary antibody conjugated to horseradish peroxidase (Jackson ImmunoResearch). Immunocomplexes were visualized using an enhanced chemiluminescence kit (ECL Plus Western blotting detection system, GE Healthcare). Protein loading was verified by probing against beta-actin (A5441, mouse, 1:5000, Sigma).

Indirect immunofluorescence microscopy

Embryos were embedded using optimal cutting temperature compound (OCT; Tissue-Tek), frozen, sectioned and fixed in 4% formaldehyde solution. Alternatively, embryos were fixed in Bouin's solution, mounted in paraffin, sectioned and antigen retrieved using 10 mM sodium citrate buffer pH 6.0. hESCs were fixed using either cold methanol or 4% paraformaldehyde. Sorted E11 *K14H2-BGFP* surface epithelium cells (described above) were cytospun onto glass slides and fixed using 4% paraformaldehyde. When applicable, the M.O.M. kit (Vector Labs) was used to prevent nonspecific binding with mouse antibodies. The following antibodies and dilutions were used for immunostaining: keratin 14 (rabbit, 1:1000, gift from J. Segre lab), keratin 14 (chicken, 1:500, gift from J. Segre lab), keratin 18 (MAB3234, mouse, 1:100, Millipore), p63 (P3362, mouse, 1:300, Sigma), p63 (ab97865, rabbit, 1:250, Abcam), Notch1 (ab27526, rabbit, 1:250, Abcam), Notch4 (N5163, rabbit, 1:250, Sigma), OCT4 (human, 1:300, Millipore) and pSMAD1/5/8 (9511S, rabbit, 1:100, Cell Signaling). Cells were stained with the appropriate fluorophore conjugated secondary antibody (Invitrogen) and mounted in ProLong Gold antifade reagent with DAPI for DNA visualization (Invitrogen).

To detect cleaved Notch1 and p63 at E10/E11, embryos were processed for immunocytochemistry using cleaved Notch1 (Val 1774-D3B8) (4147, rabbit, 1:100, Cell Signaling) and p63 (described above) antibodies. Embryo sections were fixed in 4% paraformaldehyde solution or Bouin's solution, blocked in TNB solution (TSA Fluorescence Systems Tyramide Signal Amplification kit, PerkinElmer) and incubated overnight with primary antibodies (described above). Primary antibodies were detected with appropriate fluorophore diluted in Dako EnVision+ anti-rabbit labeled polymer-HRP secondary antibody (Dako EnVision+ Dual Link System-HRP kit, Dako). The samples were incubated in tetramethylrhodamine-labeled tyramide reagent (PerkinElmer Life Sciences) and mounted as previously described. Slides were analyzed using a Zeiss Imager.M1 fluorescent microscope (Zeiss) and images were acquired with a color AxioCam MR3 camera (Zeiss).

Quantitative reverse transcription-PCR

Real-time PCR was performed as described (Festa et al., 2011). Briefly, total RNAs were isolated with Trizol (Invitrogen) and RNeasy kit (Qiagen) from FACS-sorted embryonic non-neural ectoderm, embryonic keratinocytes and from plated undifferentiated or differentiated hESCs. To generate cDNA, equal amounts of total RNA (500 ng) were added to reverse transcriptase reaction mix (Stratagene) with oligo-dT(12) as primer. Quantitative real-time PCR was conducted with a LightCycler system (Roche Diagnostics, Basel, Switzerland) using the LightCycler DNA master SYBR Green kit for 45 cycles. Primers used in these experiments are listed in supplementary material Tables S1 and S2. LightCycler analysis software was used for quantifications. The number of cycles required to reach the crossing point for each sample was used to calculate the amount of each product using the $2^{-\Delta\Delta Ct}$ method. Levels of PCR product were normalized to β-actin mRNA levels.

Statistics

To determine significance between groups, comparisons were made using Students *t*-tests with GraphPad Prism version for Macintosh (GraphPad Software). For all statistical tests, $P<0.05$ was accepted for statistical significance.

RESULTS

Induction of ectoderm specification in human embryonic stem cells

To define novel mechanisms that drive ectoderm development to the keratinocyte fate, we used a previously defined protocol to

generate ectodermal cells with the potential to form keratinocytes from hESCs (Aberdam et al., 2008). We treated H1 hESCs with BMP4 for 3 days followed by serum for 7 days (Aberdam et al., 2008). The specification of hESCs to an ectodermal cell fate was analyzed by immunofluorescence and revealed the transition of undifferentiated cells, expressing the pluripotent marker OCT4 (POU5F1) at day 0 to differentiated K18-expressing cells (Fig. 1A,B). Quantitative real-time PCR confirmed these results and showed that the levels of *OCT4* mRNA decrease following BMP4 and serum treatment and that the mRNA levels of *K18* significantly increased during differentiation (supplementary material Fig. S1). Differentiation was also accompanied by an increase in the mRNA levels of the ectodermal markers *MSX2*, *GATA2* and *GBX2* (Fig. 1D) (Davidson, 1995; Li et al., 2009; Orford et al., 1998; Schlosser and Ahrens, 2004), further indicating that ectodermal fate was induced in hESCs. At the end of the differentiation protocol, a small percentage of cells differentiated to the epidermal keratinocyte lineage, as indicated by the presence of $K14^+$ cells (Fig. 1B) (Aberdam et al., 2008) and by the increase in the levels of *K14* mRNA (supplementary material Fig. S1). These results were further confirmed by FACS and clearly show that the majority of differentiated cells are $K18^+$, whereas only 4% of the cells express K14 (Fig. 1C).

To fully characterize hESC differentiation in the presence of BMP4 and serum, we analyzed cell fates other than surface ectoderm. Endoderm or neuroectoderm lineages were not specified in BMP4/serum-treated hESCs as assayed by quantitative real-time PCR for mRNA levels of key markers *FOXA2* and *SOX1*, respectively (Fig. 1E). BMP4 treatment also activated *CDX2* mRNA and protein expression (Fig. 1E, Fig. 2C; supplementary material Fig. S10A,B), indicative of mesoderm (Bernando et al., 2011) or trophectoderm (Xu et al., 2002) specification. Taken together these results suggest that this differentiation protocol generates primarily ectodermal cells, including epidermal keratinocyte progenitor cells.

p63 is expressed before K14 during ectoderm development

To further characterize keratinocyte formation during hESC differentiation, we analyzed the expression of P63, which is expressed in stratified epithelial cells of the thymus and skin (Koster and Roop, 2007; Senoo et al., 2007) and during ectoderm specification in mouse ESCs (Medawar et al., 2008). A small percentage of $P63^+$ cells were present at the end of the differentiation protocol (Fig. 2A). Quantitative real-time analysis of mRNA expression of all P63 isoforms throughout the differentiation protocol revealed a significant upregulation of *P63* mRNA levels (Fig. 2B). Colocalization of P63 with K18, K14 and CDX2 revealed that at the end of the differentiation protocol, almost all of the $P63^+$ cells are $K18^+$ with only a small percentage of the $P63^+$ cells expressing K14 (Fig. 2C,D). As murine trophoblast lineage cells can express p63 (Shih and Kurman, 2004), we analyzed whether $P63^+$ cells expressed CDX2. We did not detect cells that co-express P63 and CDX2 in ectoderm-specified hESCs (Fig. 2C,D). Taken together, these data indicate that during hESC-induced ectoderm specification the majority of $P63^+$ cells express K18 and few cells express K14.

To test the ability of ectoderm-specified hESCs to generate keratinocytes, we cultured hESCs after BMP4/serum treatment in keratinocyte media and analyzed K14 and P63 expression by immunofluorescence. As shown above, few differentiated hESCs co-expressed P63 and K14 in BMP4/serum media (Fig. 2E,F). By contrast, after transferring the cells to keratinocyte media, 80% of $P63^+$ cells express K14 after 16 days and ~100% express K14 after 23 days (Fig. 2E,F). In addition, the number of colonies expressing P63 containing both $K14^+$ and $K14^-$ cells decreased from 34% after

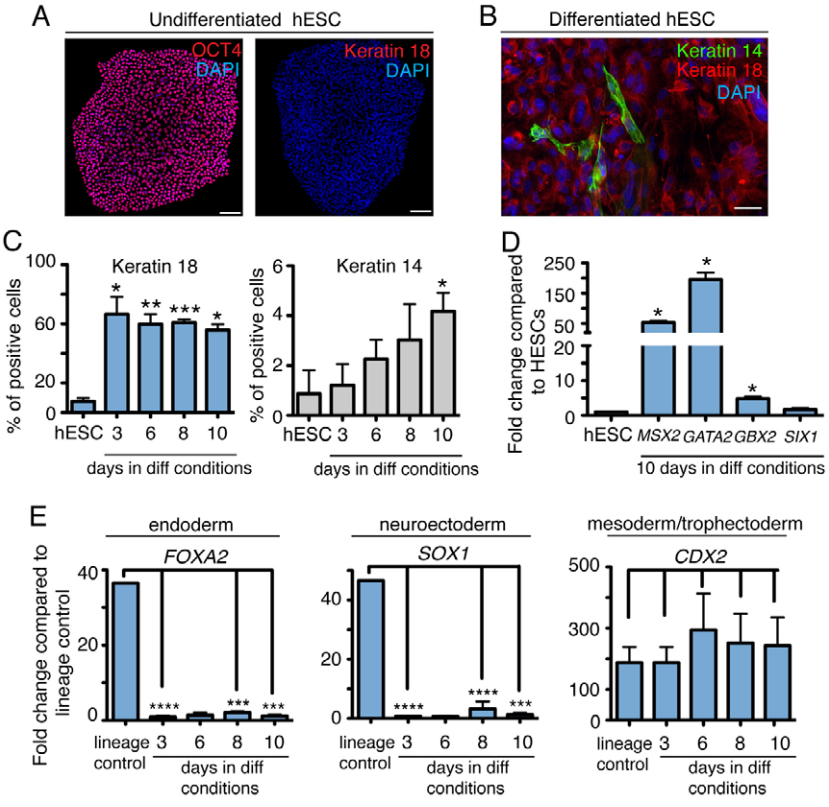

Fig. 1. Ectoderm specification in hESCs.
(**A**) Undifferentiated hESCs are positive for OCT4 (red) and negative for K18 as assayed by immunofluorescence. (**B**) Following treatment of hESCs with 0.5 nM BMP4 for 3 days and serum for 7 days, the majority of the cells are positive for K18 (red) and a small percentage of the cells are positive for K14 (green). (**C**) Analysis of K14 and K18 protein levels during ectoderm specification of hESCs as assayed by FACS (n=4-6 independent experiments for each bar). (**D**) Quantitative real-time analysis of the levels of several ectoderm markers after ectoderm specification of hESCs (n=3 independent differentiation experiments for each graph). (**E**) Ectoderm specification does not induce endoderm or neuroectoderm lineage specification as indicated by quantitative real-time PCR analysis of *FOXA2* or *SOX1* expression, respectively. Analysis of mRNA levels of *CDX2* indicates that mesoderm/trophectoderm development was initiated (n=3 independent differentiation experiments for each graph bar). All data are ± s.d. (***/****P<0.001, **0.001<P<0.01, *0.01<P<0.05). Scale bars: 100 μm in A; 50 μm in B.

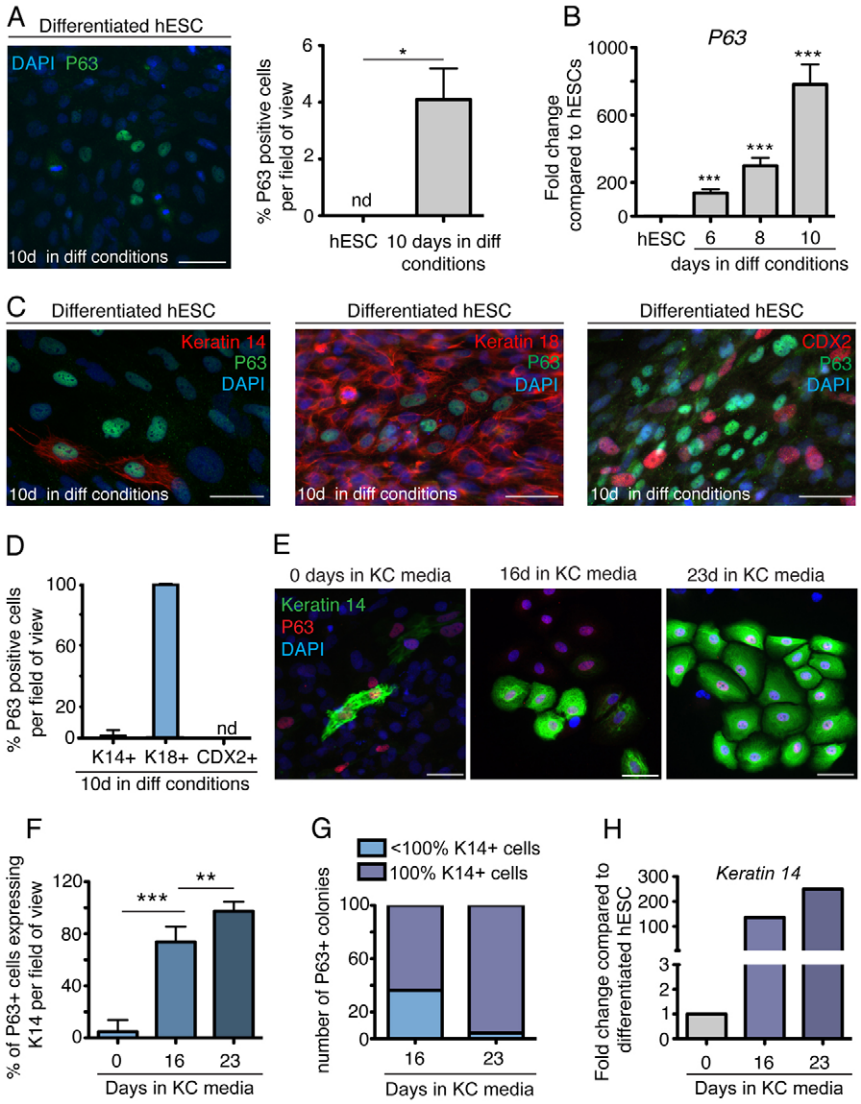

Fig. 2. P63 expression during ectoderm and keratinocyte differentiation of hESCs.
(**A**) Ectoderm-specified hESCs express P63 (green) (n=38 fields of view containing 1.65×10^4-2.0×10^4 cells from three independent experiments). (**B**) Real-time PCR analysis of mRNA levels of *P63* during differentiation compared to undifferentiated hESCs (n=9 independent differentiation experiments for each bar). (**C**) Ten days after ectoderm specification of hESCs, $P63^+$ cells (green) express K14 (red) and K18 (red) but are negative for CDX2 (red). (**D**) Quantification of the percentage of $P63^+$ cells that are positive for K14, K18 or CDX2 (n=38 fields of view containing 1.65×10^4-2.0×10^4 cells from three independent experiments). (**E**) Ectoderm-specified hESCs after 10 days of differentiation were plated in keratinocyte (KC) media for indicated time points and assayed by immunofluorescence for the presence of P63 (red) and K14 (green). (**F**) Quantification of the percentage of $P63^+/K14^+$ cells revealed an increase in the number of keratinocytes after 16 and 23 days in culture with keratinocyte medium (n=10 fields of view containing 200-792 $P63^+$ cells). (**G**) The number of colonies containing 100% $P63^+/K14^+$ increased after 23 days in culture with keratinocyte medium (n=10 fields of view containing 200-792 $P63^+$ cells). (**H**) Quantification of the mRNA levels of *K14* after plating ectoderm-specified hESCs in keratinocyte medium. All data are ± s.e.m. (***/****P<0.001, **0.001<P<0.01, *0.01<P<0.05). nd, not detected. Scale bars: 50 μm.

16 days in keratinocyte media to 4% after 23 days (Fig. 2G). This increase in epidermal keratinocyte specification was associated with a corresponding increase in *K14* mRNA when ectoderm specified hESCs are cultured 16 and 23 days in keratinocyte media compared with cells before culturing in KC media (Fig. 2H). These data support the ability of ectoderm-specified hESCs to generate epidermal lineages.

Our results examining ectoderm specification of hESCs suggest that p63 may be expressed before K14 during epidermal development, thus we analyzed p63 expression *in vivo* from E10 to E12 in wild-type murine ectoderm. At these developmental stages, the percentages of $p63^+/K14^+$ cells increased from E10 to E12. At E12 the majority of the $p63^+$ cells express K14 (Fig. 3A), indicating a full commitment to the epidermal lineage. A similar sequence of p63 expression was seen in mouse embryos that express the histone H2B tagged with GFP driven by the *K14* promoter (*K14-H2BGFP*) (Tumbar et al., 2004) (Fig. 3B). By contrast, we found that the majority of the $p63^+$ cells also express K18 throughout the embryo at E10 (Fig. 3C). As epidermal development proceeds, the majority of $p63^+$ cells lose K18 expression throughout the epithelium (Fig. 3C). These data further indicate that p63 is expressed before final keratinocyte commitment during murine development, similar to the sequence of events during ectoderm specification of hESCs.

Notch signaling is inactivated during epidermal development

Notch signaling is involved in cell-fate specification in many tissues and has been shown to repress p63 expression in fully committed epidermal keratinocytes (Nguyen et al., 2006). To determine whether Notch signaling is involved in the early events of keratinocyte specification in the developing ectoderm, we sought to analyze mRNA expression of Notch signaling components and target genes in developing keratinocytes of mouse embryos. To purify developing keratinocytes from the surface ectoderm we analyzed *K14-H2BGFP* mice, which displayed GFP^+ and GFP^- cells in the developing epidermis (supplementary material Fig. S2). At E11, a subset of GFP^+ cells express K14 or K18 and the majority of $K18^+$ cells in the developing ectoderm are GFP^- (supplementary material Fig. S2B,C). To further characterize developing keratinocytes in the surface ectoderm, individual cells were dissociated from E11 *K14-H2BGFP* embryos and immunostained with antibodies against α6 integrin and E-cadherin, which colocalize in the surface ectoderm but not in other embryonic regions

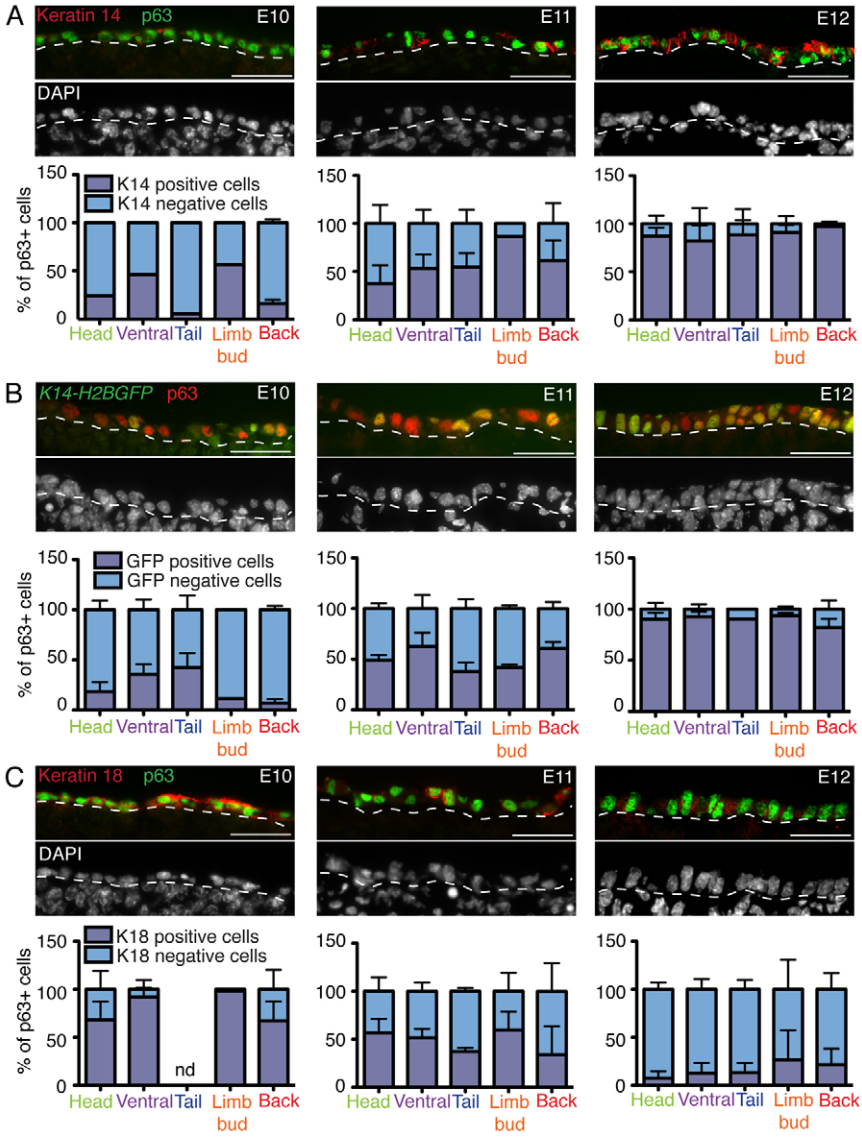

Fig. 3. p63 expression during murine keratinocyte development. (**A**) Immunofluorescence analysis of K14 (red) and p63 (green) expression during murine skin development at E10-E12. Quantification of the percentage of $p63^+$ cells that are $K14^+$ or $K14^-$ at E10-E12 in indicated regions of the embryo (*n*=3 embryos per bar). (**B**) Immunofluorescence analysis of p63 (red) expression in *K14-H2BGFP* mice during murine skin development at E10-E12. Quantification of the percentage of $p63^+$ cells that are GFP^+ or GFP^- at E10-E12 in indicated regions of the embryo (*n*=3 embryos per bar). (**C**) Immunofluorescence analysis of K18 (red) and p63 (green) expression during murine skin development at E10-E12. Quantification of the percentage of $p63^+$ cells that are $K18^+$ or $K18^-$ at E10-E12 in indicated regions of the embryo (*n*=3 embryos per bar). The dotted line indicates surface epithelium boundary. nd, not determined. Scale bars: 50 μm.

(supplementary material Fig. S3, Fig. S4A). Of the FACS-purified GFP^- cells, 100% expressed $K18^+$ and lacked K14, whereas the majority of FACS-purified GFP^+ cells were $K18^-$ and expressed K14 (supplementary material Fig. S4B). The GFP^+ cell population displayed elevated expression of *K14* and *p63* mRNAs, whereas the GFP^- population expressed higher levels of the ectodermal genes *Gata2*, *Gbx2* and *Six1* (Li et al., 2009; Orford et al., 1998; Schlosser and Ahrens, 2004) (Fig. 4A,B). Taken together, these data suggest that GFP expression can be used to analyze different stages of epidermal keratinocyte specification in E11 *K14-H2BGFP* mice, with the GFP^+ cells representing a more mature epidermal keratinocyte population.

We then analyzed the expression of Notch receptors, ligands and effectors in GFP^- and GFP^+ surface ectoderm cells from E11 *K14-H2BGFP* embryos. Quantitative real-time PCR showed a significant increase in the Notch receptor *Notch4*, several Notch ligands and the Notch target genes *Hey1* and *Hes5* in GFP^- cells compared with GFP^+ cells (Fig. 4C-E). Immunostaining E10 embryos with antibodies against Notch1 and Notch4 confirmed the expression of these receptors in ectoderm progenitor cells (supplementary material Fig. S5). To confirm that Notch signaling was active in immature ectodermal cells, we immunostained E11 embryos with antibodies against the NICD and K18 or K14. Consistent with the activation of Notch target genes in GFP^- cells in E11 *K14-H2BGFP* mouse embryos, we found that activated NICD is present in $K18^+$ cells (Fig. 4F) but absent in the majority of $K14^+$ keratinocytes (Fig. 4G). Furthermore, the majority of $p63^+$ cells are $NICD^-$ at E10 and E11 (Fig. 4H,I), suggesting that Notch signaling is not activated after p63 expression is initiated in the developing ectoderm.

To determine whether Notch pathway components were expressed during ectoderm specification of hESCs, we analyzed the levels of Notch receptors and ligands by real-time PCR and found that the expression of all four Notch receptors, *NOTCH1-4*, moderately increased (~2-fold) in BMP4/serum treated cells compared with undifferentiated hESCs (Fig. 5A). The expression of the Notch ligands *Jag1*, *Jag2*, *Dll1* and *Dll4* was also elevated following differentiation (Fig. 5B). Notch signaling target genes *Hes1*, *Hey1* and *Hes5* were also upregulated at the end of BMP4/serum-induced differentiation of hESCs (Fig. 5C). Furthermore, analysis of NICD levels by western blotting supported the activation of Notch signaling during ectoderm specification of hESCs (Fig. 5D). Taken together, these results demonstrate that Notch signaling components are present and active during ectoderm specification of hESCs similar to surface ectoderm development *in vivo*.

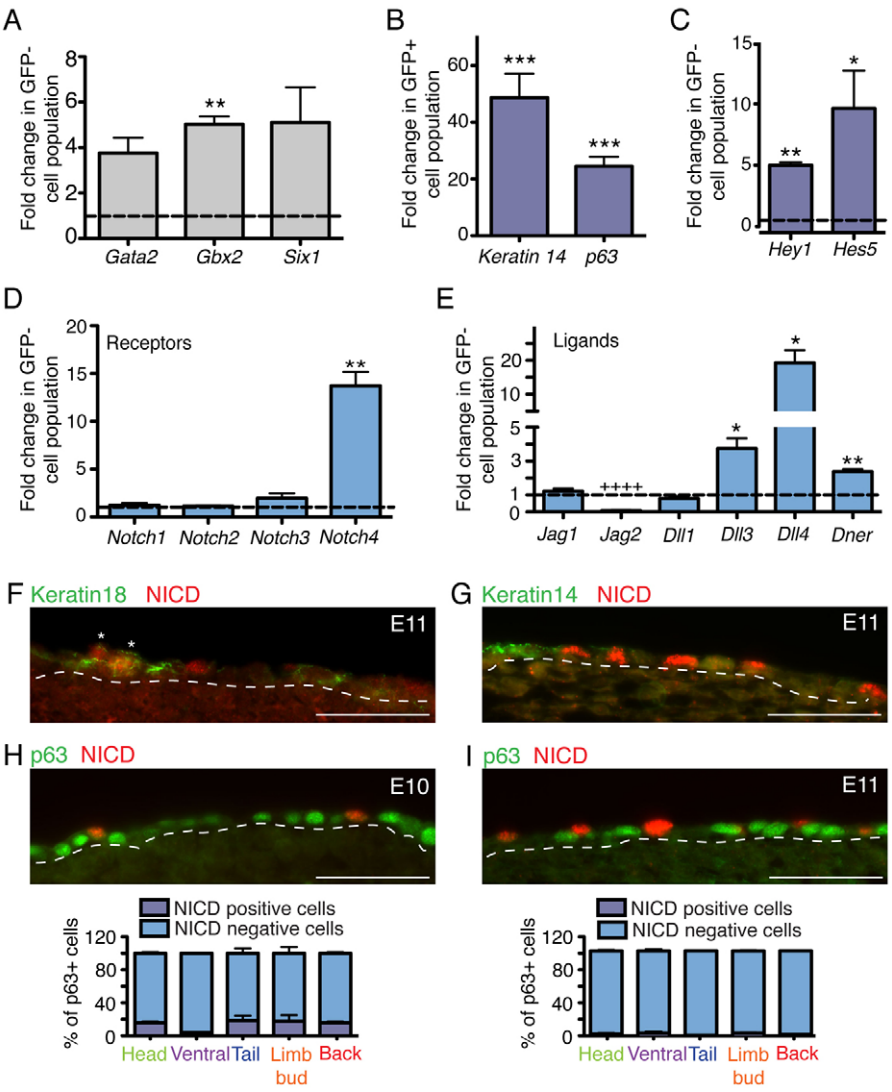

Fig. 4. Notch signaling is activated in ectodermal progenitor cells during development. (**A**) Quantitative real-time PCR analysis shows upregulation of the ectoderm markers *Gata2*, *Gbx2* and *Six1* mRNA levels in E-cadherin$^+$, α6 integrin$^+$, GFP$^-$ cells (n=3 independent FACS-purified cell populations for each bar). (**B**) Quantitative real-time PCR analysis shows upregulation of *K14* and *p63* mRNA expression in FACS purified E-cadherin$^+$, α6 integrin$^+$, GFP$^+$ (n=8 independent FACS-purified cell populations for each bar). (**C**) Quantitative real-time PCR analysis of the mRNA levels of *Hey1* and *Hes5* shows an upregulation in E11 E-cadherin$^+$, α6 integrin$^+$, GFP$^-$ cells (n=8 independent FACS purified cell populations for each bar). (**D**,**E**) Quantitative real-time PCR analysis reveals an upregulation of mRNA levels of the *Notch4* receptor (D) as well as the Notch ligands *Jag1*, *Jag2*, *Dll1*, *Dll3*, *Dll4* and *DNER* (E) in E-cadherin$^+$, α6 integrin$^+$, GFP$^-$ cells at E11 (n=4 independent FACS-purified cell populations for each bar). (**F**) Notch signaling pathway is activated in K18$^+$ cells (green) as shown by immunofluorescence for the NICD (red) at E11. Asterisks indicate K18$^+$/NICD$^+$ cells. (**G**) At E11 K14+ cells (green) are negative for NICD (red). (**H**,**I**) Immunofluorescence analysis of NICD (red) and p63 (green) expression during murine skin development at E10 (H) and E11 (I). Quantification of the percentage of p63$^+$ cells that are NICD$^+$ or NICD$^-$ at E10 (H) or E11 (I) in indicated regions of the embryo (n=3 embryos per bar). All data are ± s.d. (^{++++}P<0.001, $^{***}P$<0.001, **0.001<P<0.01, *0.01<P<0.05). The dotted line indicates surface epithelium boundary. Scale bars: 50 μm.

Inactivation of Notch signaling promotes p63 expression in developing ectoderm

To define the role of Notch signaling during ectoderm specification, we inhibited Notch signaling with N-[N-(3,5-difluorophenacetyl)-1-alanyl]-S-phenylglycine t-butyl ester (DAPT), an inhibitor of γ-secretase, during ectoderm specification of hESCs (Dovey et al., 2001). In the presence of DAPT Notch signaling was inhibited, as indicated by the lack of NICD expression during differentiation (Fig. 6A). The inactivation of the Notch pathway was further confirmed by real-time PCR showing a significant decrease in the mRNA levels of *Hes5* in DAPT-treated cells compared with vehicle-treated cells (Fig. 6B).

To analyze ectoderm specification in DAPT-treated cells, we analyzed mRNA expression of *K18* and *Cdx2* by real-time PCR. The expression of *K18* mRNA or protein was not significantly altered during differentiation in the presence of DAPT (supplementary material Figs S6, S7, S9). Despite previous reports that inhibition of Notch signaling can promote trophoblast differentiation of hESCs in embryoid bodies (Yu et al., 2008), trophoblast differentiation was not altered by DAPT treatment of hESCs during ectoderm specification as indicated by similar levels of CDX2 protein and mRNA levels in DAPT-treated hESCs compared with untreated or vehicle-treated cells (supplementary material Fig. S10A,B).

Next, we examined the effect of inhibiting Notch signaling on epidermal keratinocyte specification in hESCs. DAPT-treated hESCs displayed significantly elevated levels of *P63* mRNA at 6, 8 and 10 days following differentiation (Fig. 6B). Immunostaining with antibodies against P63 confirmed an increase in the number of P63$^+$ cells in DAPT-treated cultures compared with those treated with a vehicle control (Fig. 6C,D). To determine whether the increase of P63$^+$ cells with DAPT treatment was due to the promotion of committed trophoblasts or fully committed epidermal keratinocytes, we analyzed whether the increased number of P63$^+$ cells also expressed CDX2 or K14, respectively. After DAPT treatment, we did not detect CDX2$^+$/P63$^+$ cells (supplementary material Fig. S10A) and the percentage of K14$^+$/P63$^+$ cells was not changed (Fig. 6D; supplementary material Fig. S8). Moreover, *K14* mRNA expression was not altered by DAPT treatment of hESCs during ectoderm specification (supplementary material Fig. S6). However, DAPT-treated cultures displayed an increase in the percentage of K18$^+$/P63$^+$ cells (supplementary material Fig. S9), indicating that Notch signaling represses P63 expression in ectodermal cells.

To determine whether Notch signaling plays a role in p63 expression in developing ectoderm *in vivo*, we examined mice lacking expression of presenilin 1 and 2 (*Psen1* and *Psen2* – Mouse

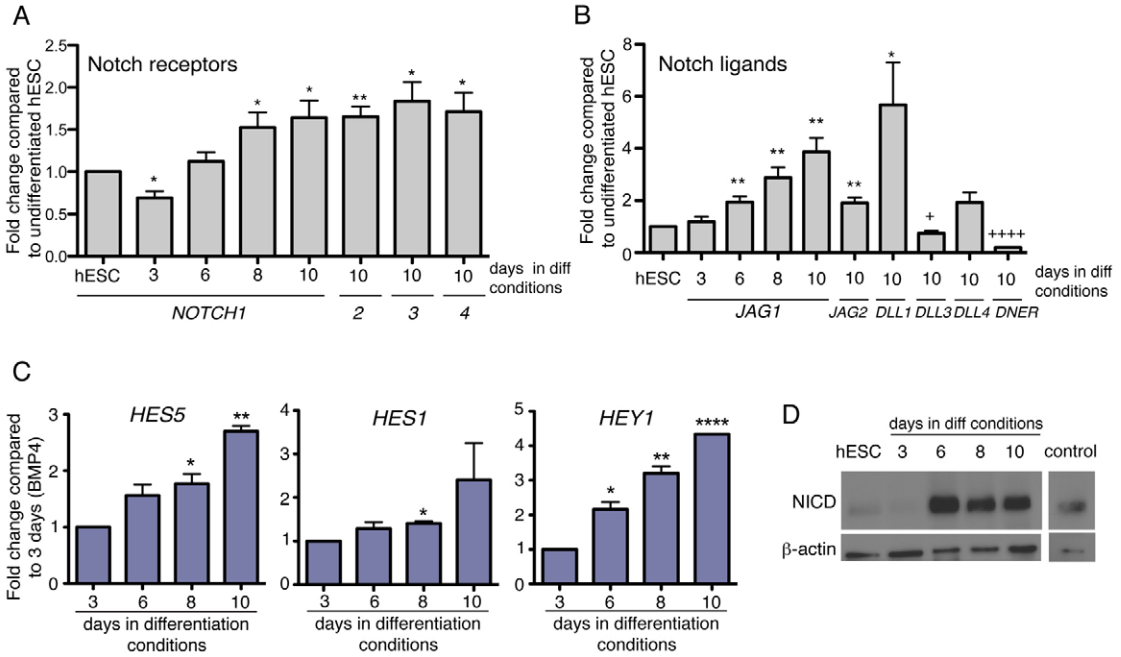

Fig. 5. Notch signaling is activated during ectoderm specification in hESCs. (**A**,**B**) Quantitative real-time PCR analysis of mRNA levels of all four Notch receptors (*NOTCH1-4*) and ligands *JAG1*, *JAG2*, *DLL1*, *DLL3*, *DLL4* and *DNER* in differentiated hESCs at indicated days after induction compared with undifferentiated cells. (**C**) Quantitative real-time PCR analysis of mRNA levels of *HES1*, *HES5* and *HEY1* indicates activation of Notch signaling in differentiated hESCs. (**D**) Notch signaling pathway is activated during ectoderm specification of hESCs as shown by western blot for NICD. Western blot for β-actin was carried out as a loading control. The positive control sample is protein from P0 murine kidney (all quantitative real-time PCR analyses are n=6 independent differentiation experiments for each bar). All data are ± s.d. ($^{++++/****}P<0.001$, $^{**}0.001<P<0.01$, $^{*}0.01<P<0.05$).

Genome Informatics; *PS* null mice), which produces the catalytic site of γ-secretase (Mizutani et al., 2001; Pan et al., 2004; Saxena et al., 2001). *PS* null mice lack Hes5 expression, supporting the abrogation of Notch signaling, and display several developmental defects resulting in embryonic lethality after E9.5 (Donoviel et al., 1999). Thus, we analyzed whether the loss of Notch signaling in *PS* null mice at E9.5 results in precocious expression of p63. In control embryos ($PS1^{f/f};PS2^{-/-}$), few cells express p63 at E9.5; however, *PS* null mice display a significant upregulation of p63 expression in the surface ectoderm (Fig. 6E,F). We did not detect elevated K14 expression (data not shown), which indicates that loss of Notch did not accelerate complete epidermal commitment at E9.5. Taken together, these data are consistent with our results in hESCs and suggest that Notch signaling *in vivo* represses the expression of p63 during the development of surface ectoderm.

To determine whether Notch signaling represses P63 expression during active BMP signaling or following BMP4-mediated ectoderm induction, we treated hESCs with DAPT either during BMP treatment (days 1-3) or following BMP4 addition (days 4-10) (supplementary material Fig. S11A) and analyzed *HES5* and *P63* expression by quantitative real-time PCR. Inhibition of Notch signaling reduced *HES5* mRNA levels at either treatment time point (supplementary material Fig. S11B) and did not alter phosphorylated SMAD levels during ectoderm specification (supplementary material Fig. S11D). DAPT treatment during the BMP4 treatment but not following BMP4 addition significantly increased P63 levels (supplementary material Fig. S11C). These data suggest that P63 expression is induced by inhibition of Notch signaling and active BMP4 signaling, which is consistent with the upregulation of *P63* mRNA after BMP4 addition (Medawar et al., 2008) and the inability of p63 overexpression to induce keratinocyte formation in the absence of BMP4 addition in mouse ESCs (Medawar et al., 2008).

DISCUSSION

Based on the timing of p63 expression in the developing ectoderm, we propose that p63 is expressed in pre-epidermal keratinocytes that will generate bona fide $K14^{+}$ epidermal keratinocytes in the developing surface ectoderm (Fig. 7). Our model is consistent with the ability of p63 to directly regulate K14 expression (Romano et al., 2009), the absence of K14 expression in mice and hESCs lacking p63 isoforms (Mills et al., 1999; Romano et al., 2012; Shalom-Feuerstein et al., 2011; Yang et al., 1999) and the expression of p63 as early as E9.5 in mouse embryos (Koster and Roop, 2004). Given the predominant expression of ΔNp63 in physiologically normal epidermal tissues and the requirement of ΔNp63 for epidermal development (Romano et al., 2009), ΔNp63 is likely to be the isoform expressed in the surface ectoderm. Future studies analyzing p63 isoform expression in the surface ectoderm and the lineage commitment of p63-expressing ectodermal cells will further reveal the contribution of these cells to keratinocyte formation.

Notch signaling has been shown to be important for the commitment of basal keratinocytes to terminal differentiation during development (Blanpain et al., 2006; Moriyama et al., 2008; Nguyen et al., 2006; Pan et al., 2004). Although several groups have deleted Notch signaling components and analyzed keratinocyte defects, alterations in epidermal specification have not been noted to date. As the four Notch receptors and ligands are redundant (Kitamoto et al., 2005; Krebs et al., 2000; Pan et al., 2004), several receptors or ligands must be deleted simultaneously to generate phenotypes in many systems. Additionally, conditional deletion of Notch components within the skin has been performed

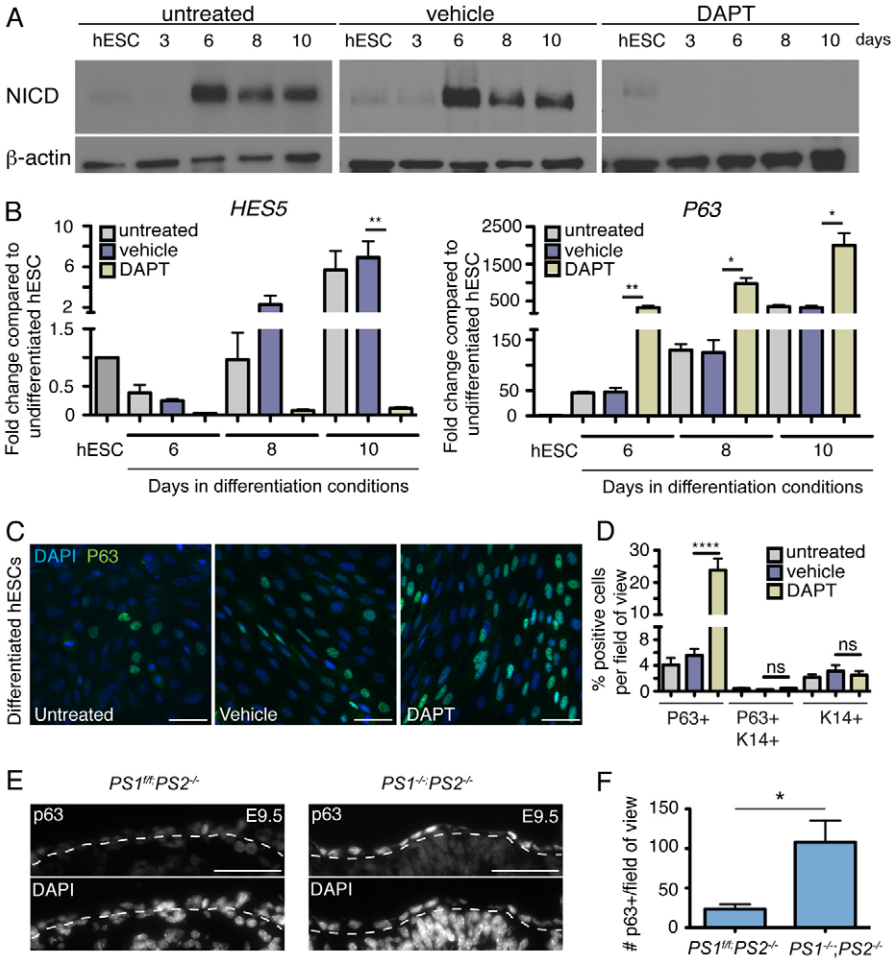

Fig. 6. Inactivation of Notch signaling promotes p63 expression during ectoderm specification. (**A**) hESCs were treated with the γ-secretase inhibitor DAPT during ectoderm differentiation. Inactivation of the Notch signaling pathway was confirmed by the absence of NICD by western blot analysis. Western blot for β-actin was carried out as a loading control. (**B**) Quantitative real-time PCR analysis of mRNA levels of *HES5* and *P63* in untreated, vehicle- or DAPT-treated hESCs during ectoderm differentiation (*n*=5 independent differentiation experiments for each graph bar). (**C**) Untreated, vehicle- and DAPT-treated hESCs after 10 days of ectoderm specification were immunostained for P63 (green). (**D**) Quantification of the number of $P63^+$, $K14^+$ cells or $P63^+/K14^+$ cells in untreated, vehicle- and DAPT-treated hESCs after 10 days of ectoderm specification (*n*=38 fields of view containing 1.65×10^4-2.0×10^4 cells from three independent experiments). ns, not significant. (**E**) Sections of control ($PS1^{f/f};PS2^{-/-}$) or *PS* null ($PS^{-/-};PS2^{-/-}$) embryos at E9.5 were stained with antibodies against p63. (**F**) Quantification of p63 cells per field of view (*n*=3-5 embryos per bar). For B, data are ± s.d. (**0.001<*P*<0.01,*0.01<*P*<0.05), for D and F data are ± s.e.m. (****P<0.001,*0.01<P<0.05). The dotted line indicates the surface epithelium boundary. Scale bars: 50 μm.

using keratin promoters, which act after p63 expression is initiated (Blanpain et al., 2006; Demehri and Kopan, 2009). Interestingly, *Presenilin* genes have been conditionally deleted in a mosaic pattern within the surface ectoderm using mice expressing Cre driven by the *Msx2* promoter, which is active around E9.5, but the expression of p63 was not examined in these mice (Pan et al., 2004). Whether the activity of the *Msx2* promoter would allow manipulation of genes in the pre-keratinocyte phase of surface ectoderm development will be an interesting avenue of future investigation.

By taking advantage of the specification of hESCs to ectodermal lineages and complete ablation of Notch signaling within embryos, we were able to identify a role for Notch signaling in the regulation of p63 expression during ectoderm specification. Our data are consistent with the ability of activated Notch1 to repress p63 expression in fully committed keratinocytes (Nguyen et al., 2006).

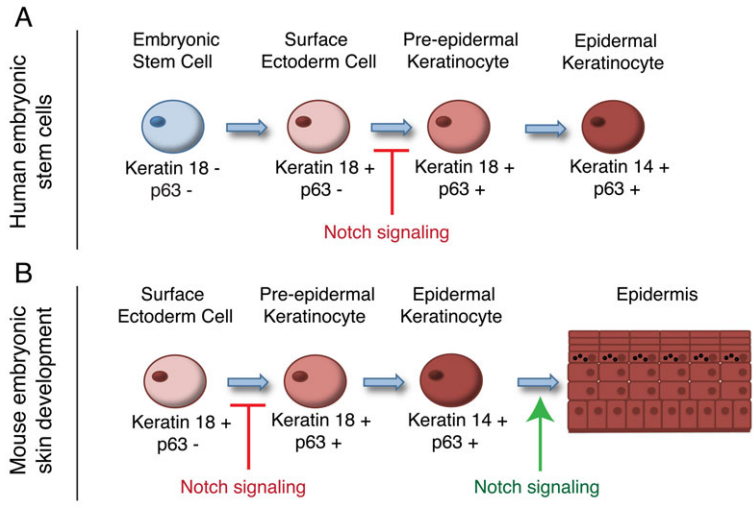

Fig. 7. Model for keratinocyte specification during epidermal development. Keratinocyte specification occurs in multiple steps during (**A**) *in vitro* differentiation of hESCs and during (**B**) *in vivo* murine skin development. Surface ectoderm progenitor cells express K18 and display activated Notch signaling. Upon release of Notch signaling, $K18^+$ cells upregulate p63 expression to initiate keratinocyte lineage commitment. $p63^+$ cells express K14 to generate a fully committed keratinocyte, which upon later Notch signals promote stratification and the formation of the mature epidermis.

The inhibition of p63 expression in ectoderm progenitors suggests that, like in muscle, neuron and hepatocyte fate decisions, Notch signaling represses keratinocyte fate during development (Han et al., 2011; Lai, 2004). This idea is consistent with previous studies in *Xenopus* embryos demonstrating that activated Notch expression can inhibit epidermal keratin gene expression (Coffman et al., 1993). As this previous study expressed activated Notch in 2- to 8-cell embryos, the direct role of Notch signaling in surface ectoderm was not defined. Our data extend this finding to implicate Notch signaling in keratinocyte specification in higher vertebrates, and demonstrate that Notch signaling acts in surface ectoderm cells to repress *p63* expression.

Notch signaling may activate p63 expression via several mechanisms. NICD activation could activate RBP-Jk to directly activate the *p63* promoter, which contains putative RBP-Jk binding sites (data not shown). Alternatively, non-canonical Notch signaling may be involved by interacting with alternative signaling pathways such as FGF, Shh and Wnt signaling (Sanalkumar et al., 2010). Non-canonical Notch signaling in the skin occurs given the different phenotypes of conditional genetic mouse models lacking a functional γ-secretase complex (presenelin 1/2; PS1/PS2), the Notch receptors (Notch1/2; N1/N2) or the RBP-Jk transcriptional repressor (Demehri and Kopan, 2009). In a similar fashion, p63 may negatively regulate Notch signaling pathway. In fact, mouse embryos lacking *ΔNp63* display defects in Notch signaling, and *ΔNp63* directly binds to the promoters of Notch1 (Nguyen et al., 2006) and Notch3 (Romano et al., 2012). Identification of the cell types that express Notch ligands and whether the downstream targets of Notch signaling, such as Rbp-Jk or Hes5, directly control *p63* expression will be an avenue of future investigation.

The influence of Notch signaling on the timing of surface ectoderm specification may act in coordination with BMP and Wnt signaling. Our data suggest that epidermal keratinocyte specification requires active BMP4 signaling and inhibition of Notch signaling. This observation is consistent with previous studies showing that p63 induction of epidermal keratinocyte fate in mouse ESCs requires BMP4 signaling (Medawar et al., 2008). Additionally, BMP signaling can induce ectodermal fate in hESCs (Aberdam et al., 2008; Harvey et al., 2010) and in surface ectoderm progenitors of *Xenopus* embryos (Wilson and Hemmati-Brivanlou, 1995). Wnt signals can also promote surface ectoderm fate and repress neuroectoderm fate (Wilson et al., 2001). Thus, Wnt signaling may coordinate with BMP signaling to specify the surface ectoderm, whereas Notch signaling may laterally inhibit keratinocyte fate, similar to the sequence of events that control *Drosophila* peripheral nervous system development (Hayward et al., 2008). Studies to further define the timing and interactions between these signaling pathways may reveal novel aspects of the developmental sequence of keratinocyte formation.

In conclusion, our data highlight the utility of using hESCs as a model for ectoderm development. Our works supports the parallels between hESCs and ectoderm specification in murine embryos. Our concurrent analysis of developing murine embryos and ectoderm specification in hESCs allowed us to identify a novel role for Notch signaling in ectoderm specification and to further define the sequence of events that occur during keratinocyte development. Future work will show whether manipulation of Notch signaling can enhance keratinocyte formation in hESCs for therapeutic use in skin diseases and disorders.

Acknowledgements
We thank Drs Raphael Kopan, Tudorita Tumbar, Michael Rendl, Hoang Ngyuen, Matthew Rodeheffer, and Horsley lab members for critical reading of the manuscript and valuable discussions. Dr Raphael Kopan graciously provided the PS null embryos (NIH). We also thank Kan Chen for technical assistance.

Funding
This work was funded by CT Innovations [12-SCB-YALE-01]. The PS mice were provided with funding from the National Institutes of Health (NIH) [GM554709, R. Kopan PI]. A.M.B.T. was a Fundação para a Ciência e Tecnologia postdoctoral fellow. V.H. is a Pew Scholar in Biomedical Research and is funded by the NIH [AR060295]. Deposited in PMC for release after 12 months.

Competing interests statement
The authors declare no competing financial interests.

Author contributions
A.M.B.T. completed all experimental work. A.M.B.T. and V.H. designed the study, interpreted data and wrote the manuscript.

Supplementary material
Supplementary material available online at
http://dev.biologists.org/lookup/suppl/doi:10.1242/dev.093948/-/DC1

References

Aberdam, E., Barak, E., Rouleau, M., de LaForest, S., Berrih-Aknin, S., Suter, D. M., Krause, K.-H., Amit, M., Itskovitz-Eldor, J. and Aberdam, D. (2008). A pure population of ectodermal cells derived from human embryonic stem cells. *Stem Cells* **26**, 440-444.

Bernando, A. S., Faial, T., Gardner, L., Niakan, K. K., Ortmann, D., Senner, C. E., Callery, E. M., Trotter, M. W., Hemberger, M., Smith J. C. et al. (2011). BRACHYURY and CDX2 mediate BMP-induced differentiation of human and mouse pluripotent stem cells into embryonic and extraembryonic lineages. *Cell Stem Cell* **9**, 144-155.

Blanpain, C. and Fuchs, E. (2006). Epidermal stem cells of the skin. *Annu. Rev. Cell Dev. Biol.* **22**, 339-373.

Blanpain, C., Lowry, W. E., Pasolli, H. A. and Fuchs, E. (2006). Canonical notch signaling functions as a commitment switch in the epidermal lineage. *Genes Dev.* **20**, 3022-3035.

Bouras, T., Pal, B., Vaillant, F., Harburg, G., Asselin-Labat, M.-L., Oakes, S. R., Lindeman, G. J. and Visvader, J. E. (2008). Notch signaling regulates mammary stem cell function and luminal cell-fate commitment. *Cell Stem Cell* **3**, 429-441.

Byrne, C., Tainsky, M. and Fuchs, E. (1994). Programming gene expression in developing epidermis. *Development* **120**, 2369-2383.

Candi, E., Schmidt, R. and Melino, G. (2005). The cornified envelope: a model of cell death in the skin. *Nat. Rev. Mol. Cell Biol.* **6**, 328-340.

Chambers, S. M., Fasano, C. A., Papapetrou, E. P., Tomishima, M., Sadelain, M. and Studer, L. (2009). Highly efficient neural conversion of human ES and iPS cells by dual inhibition of SMAD signaling. *Nat. Biotechnol.* **27**, 275-280.

Coffman, C. R., Skoglund, P., Harris, W. A. and Kintner, C. R. (1993). Expression of an extracellular deletion of Xotch diverts cell fate in Xenopus embryos. *Cell* **73**, 659-671.

Crum, C. P. and McKeon, F. D. (2010). p63 in epithelial survival, germ cell surveillance, and neoplasia. *Annu. Rev. Pathol.* **5**, 349-371.

D'Amour, K. A., Agulnick, A. D., Eliazer, S., Kelly, O. G., Kroon, E. and Baetge, E. E. (2005). Efficient differentiation of human embryonic stem cells to definitive endoderm. *Nat. Biotechnol.* **23**, 1534-1541.

Davidson, D. (1995). The function and evolution of Msx genes: pointers and paradoxes. *Trends Genet.* **11**, 405-411.

Demehri, S. and Kopan, R. (2009). Notch signaling in bulge stem cells is not required for selection of hair follicle fate. *Development* **136**, 891-896.

Donoviel, D. B., Hadjantonakis, A. K., Ikeda, M., Zheng, H., Hyslop, P. S. and Bernstein, A. (1999). Mice lacking both presenilin genes exhibit early embryonic patterning defects. *Genes Dev.* **13**, 2801-2810.

Dovey, H. F., John, V., Anderson, J. P., Chen, L. Z., de Saint Andrieu, P., Fang, L. Y., Freedman, S. B., Folmer, B., Goldbach, E., Holsztynska, E. J. et al. (2001). Functional gamma-secretase inhibitors reduce beta-amyloid peptide levels in brain. *J. Neurochem.* **76**, 173-181.

Festa, E., Fretz, J., Berry, R., Schmidt, B., Rodeheffer, M., Horowitz, M. and Horsley, V. (2011). Adipocyte lineage cells contribute to the skin stem cell niche to drive hair cycling. *Cell* **146**, 761-771.

Fuchs, E. (2007). Scratching the surface of skin development. *Nature* **445**, 834-842.

Han, S., Dziedzic, N., Gadue, P., Keller, G. M. and Gouon-Evans, V. (2011). An endothelial cell niche induces hepatic specification through dual repression of Wnt and Notch signaling. *Stem Cells* **29**, 217-228.

Harvey, N. T., Hughes, J. N., Lonic, A., Yap, C., Long, C., Rathjen, P. D. and Rathjen, J. (2010). Response to BMP4 signalling during ES cell differentiation defines intermediates of the ectoderm lineage. *J. Cell Sci.* **123**, 1796-1804.

Hayward, P., Kalmar, T. and Arias, A. M. (2008). Wnt/Notch signalling and information processing during development. *Development* **135**, 411-424.
King, K. E. and Weinberg, W. C. (2007). p63: defining roles in morphogenesis, homeostasis, and neoplasia of the epidermis. *Mol. Carcinog.* **46**, 716-724.
Kitamoto, T., Takahashi, K., Takimoto, H., Tomizuka, K., Hayasaka, M., Tabira, T. and Hanaoka, K. (2005). Functional redundancy of the Notch gene family during mouse embryogenesis: analysis of Notch gene expression in Notch3-deficient mice. *Biochem. Biophys. Res. Commun.* **331**, 1154-1162.
Kopan, R. and Ilagan, M. X. G. (2009). The canonical Notch signaling pathway: unfolding the activation mechanism. *Cell* **137**, 216-233.
Koster, M. I. (2010). p63 in skin development and ectodermal dysplasias. *J. Invest. Dermatol.* **130**, 2352-2358.
Koster, M. I. and Roop, D. R. (2004). p63 and epithelial appendage development. *Differentiation* **72**, 364-370.
Koster, M. I. and Roop, D. R. (2007). Mechanisms regulating epithelial stratification. *Annu. Rev. Cell Dev. Biol.* **23**, 93-113.
Krebs, L. T., Xue, Y., Norton, C. R., Shutter, J. R., Maguire, M., Sundberg, J. P., Gallahan, D., Closson, V., Kitajewski, J., Callahan, R. et al. (2000). Notch signaling is essential for vascular morphogenesis in mice. *Genes Dev.* **14**, 1343-1352.
Lai, E. C. (2004). Notch signaling: control of cell communication and cell fate. *Development* **131**, 965-973.
Laurikkala, J., Mikkola, M. L., James, M., Tummers, M., Mills, A. A. and Thesleff, I. (2006). p63 regulates multiple signalling pathways required for ectodermal organogenesis and differentiation. *Development* **133**, 1553-1563.
Lechler, T. and Fuchs, E. (2005). Asymmetric cell divisions promote stratification and differentiation of mammalian skin. *Nature* **437**, 275-280.
Li, B., Kuriyama, S., Moreno, M. and Mayor, R. (2009). The posteriorizing gene Gbx2 is a direct target of Wnt signalling and the earliest factor in neural crest induction. *Development* **136**, 3267-3278.
McGowan, K. M. and Coulombe, P. A. (1998). Onset of keratin 17 expression coincides with the definition of major epithelial lineages during skin development. *J. Cell Biol.* **143**, 469-486.
Medawar, A., Virolle, T., Rostagno, P., de la Forest-Divonne, S., Gambaro, K., Rouleau, M. and Aberdam, D. (2008). DeltaNp63 is essential for epidermal commitment of embryonic stem cells. *PLoS ONE* **3**, e3441.
Metallo, C. M., Ji, L., de Pablo, J. J. and Palecek, S. P. (2008). Retinoic acid and bone morphogenetic protein signaling synergize to efficiently direct epithelial differentiation of human embryonic stem cells. *Stem Cells* **26**, 372-380.
Mills, A. A., Zheng, B., Wang, X. J., Vogel, H., Roop, D. R. and Bradley, A. (1999). p63 is a p53 homologue required for limb and epidermal morphogenesis. *Nature* **398**, 708-713.
Mizutani, T., Taniguchi, Y., Aoki, T., Hashimoto, N. and Honjo, T. (2001). Conservation of the biochemical mechanisms of signal transduction among mammalian Notch family members. *Proc. Natl. Acad. Sci. USA* **98**, 9026-9031.
Moriyama, M., Durham, A.-D., Moriyama, H., Hasegawa, K., Nishikawa, S.-I., Radtke, F. and Osawa, M. (2008). Multiple roles of Notch signaling in the regulation of epidermal development. *Dev. Cell* **14**, 594-604.
Nagarajan, P., Romano, R.-A. and Sinha, S. (2008). Transcriptional control of the differentiation program of interfollicular epidermal keratinocytes. *Crit. Rev. Eukaryot. Gene Expr.* **18**, 57-79.
Nguyen, B.-C., Lefort, K., Mandinova, A., Antonini, D., Devgan, V., Della Gatta, G., Koster, M. I., Zhang, Z., Wang, J., Tommasi di Vignano, A. et al. (2006). Cross-regulation between Notch and p63 in keratinocyte commitment to differentiation. *Genes Dev.* **20**, 1028-1042.
Orford, R. L., Robinson, C., Haydon, J. M., Patient, R. K. and Guille, M. J. (1998). The maternal CCAAT box transcription factor which controls GATA-2 expression is novel and developmentally regulated and contains a double-stranded-RNA-binding subunit. *Mol. Cell. Biol.* **18**, 5557-5566.
Pan, Y., Lin, M.-H., Tian, X., Cheng, H.-T., Gridley, T., Shen, J. and Kopan, R. (2004). gamma-secretase functions through Notch signaling to maintain skin appendages but is not required for their patterning or initial morphogenesis. *Dev. Cell* **7**, 731-743.
Romano, R.-A., Birkaya, B. and Sinha, S. (2007). A functional enhancer of keratin14 is a direct transcriptional target of deltaNp63. *J. Invest. Dermatol.* **127**, 1175-1186.
Romano, R.-A., Ortt, K., Birkaya, B., Smalley, K. and Sinha, S. (2009). An active role of the DeltaN isoform of p63 in regulating basal keratin genes K5 and K14 and directing epidermal cell fate. *PLoS ONE* **4**, e5623.
Romano, R.-A., Smalley, K., Magraw, C., Serna, V. A., Kurita, T., Raghavan, S. and Sinha, S. (2012). ΔNp63 knockout mice reveal its indispensable role as a master regulator of epithelial development and differentiation. *Development* **139**, 772-782.
Sanalkumar, R., Dhanesh, S. B. and James, J. (2010). Non-canonical activation of Notch signaling/target genes in vertebrates. *Cell. Mol. Life Sci.* **67**, 2957-2968.
Sanes, J. R., Rubenstein, J. L. and Nicolas, J. F. (1986). Use of a recombinant retrovirus to study post-implantation cell lineage in mouse embryos. *EMBO J.* **5**, 3133-3142.
Saura, C. A., Choi, S.-Y., Beglopoulos, V., Malkani, S., Zhang, D., Shankaranarayana Rao, B. S., Chattarji, S., Kelleher, R. J., 3rd, Kandel, E. R., Duff, K. et al. (2004). Loss of presenilin function causes impairments of memory and synaptic plasticity followed by age-dependent neurodegeneration. *Neuron* **42**, 23-36.
Saxena, M. T., Schroeter, E. H., Mumm, J. S. and Kopan, R. (2001). Murine notch homologs (N1-4) undergo presenilin-dependent proteolysis. *J. Biol. Chem.* **276**, 40268-40273.
Schlosser, G. and Ahrens, K. (2004). Molecular anatomy of placode development in Xenopus laevis. *Dev. Biol.* **271**, 439-466.
Senoo, M., Pinto, F., Crum, C. P. and McKeon, F. (2007). p63 Is essential for the proliferative potential of stem cells in stratified epithelia. *Cell* **129**, 523-536.
Shalom-Feuerstein, R., Lena, A. M., Zhou, H., De La Forest Divonne, S., Van Bokhoven, H., Candi, E., Melino, G. and Aberdam, D. (2011). ΔNp63 is an ectodermal gatekeeper of epidermal morphogenesis. *Cell Death Differ.* **18**, 887-896.
Shih, I. M. and Kurman, R. J. (2004). p63 expression is useful in the distinction of epithelioid trophoblastic and placental site trophoblastic tumors by profiling trophoblastic subpopulations. *Am. J. Surg. Pathol.* **28**, 1177-1183.
Truong, A. B. and Khavari, P. A. (2007). Control of keratinocyte proliferation and differentiation by p63. *Cell Cycle* **6**, 295-299.
Tumbar, T., Guasch, G., Greco, V., Blanpain, C., Lowry, W. E., Rendl, M. and Fuchs, E. (2004). Defining the epithelial stem cell niche in skin. *Science* **303**, 359-363.
Wilson, P. A. and Hemmati-Brivanlou, A. (1995). Induction of epidermis and inhibition of neural fate by Bmp-4. *Nature* **376**, 331-333.
Wilson, S. I., Rydström, A., Trimborn, T., Willert, K., Nusse, R., Jessell, T. M. and Edlund, T. (2001). The status of Wnt signalling regulates neural and epidermal fates in the chick embryo. *Nature* **411**, 325-330.
Xu, R. H., Chen, X., Li, D. S., Li, R., Addicks, G. C., Glennon, C., Zwaka, T. P. and Thomson, J. A. (2002). BMP4 initiates human embryonic stem cell differentiation to trophoblast. *Nat. Biotechnol.* **20**, 1261-1264.
Yang, A., Schweitzer, R., Sun, D., Kaghad, M., Walker, N., Bronson, R. T., Tabin, C., Sharpe, A., Caput, D., Crum, C. et al. (1999). p63 is essential for regenerative proliferation in limb, craniofacial and epithelial development. *Nature* **398**, 714-718.
Yu, X., Zou, J., Ye, Z., Hammond, H., Chen, G., Tokunaga, A., Mali, P., Li, Y.-M., Civin, C., Gaiano, N. et al. (2008). Notch signaling activation in human embryonic stem cells is required for embryonic, but not trophoblastic, lineage commitment. *Cell Stem Cell* **2**, 461-471.

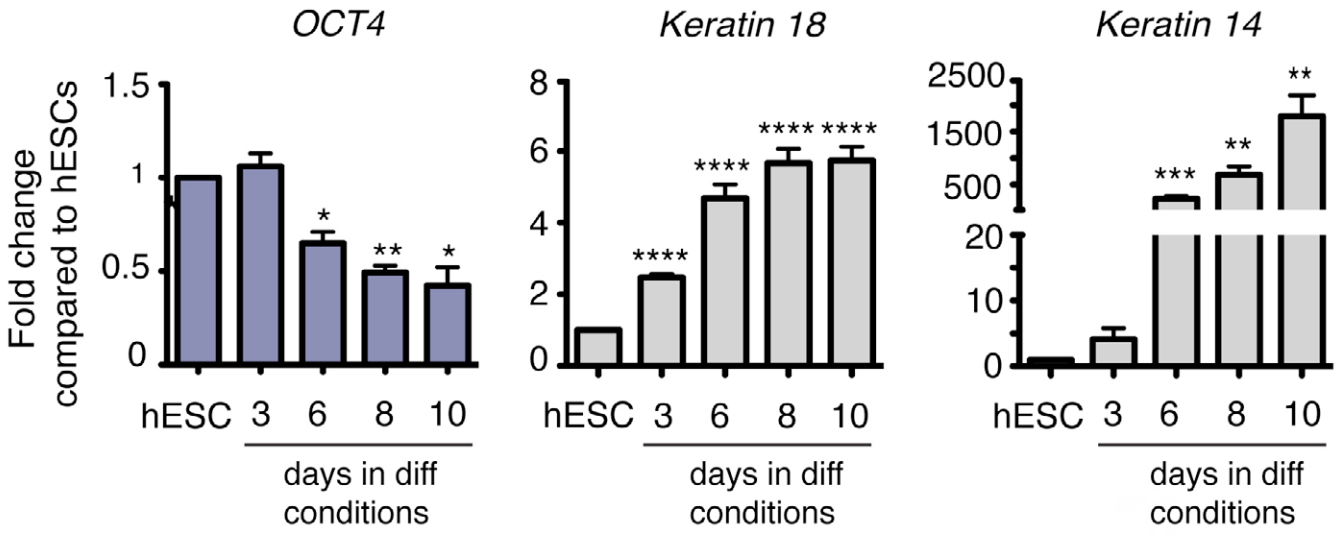

Fig. S1. Upregulation of *K18* and *K14* mRNA levels during ectoderm specification of hESCs. Quantitative real-time PCR analysis of mRNA levels of *OCT4* (*n*=3 independent differentiation experiments for each bar), *K18* and *K14* (*n*=9 independent differentiation experiments for each bar) during hESC ectoderm specification shows a downregulation of the pluripotency marker and an upregulation of keratins.

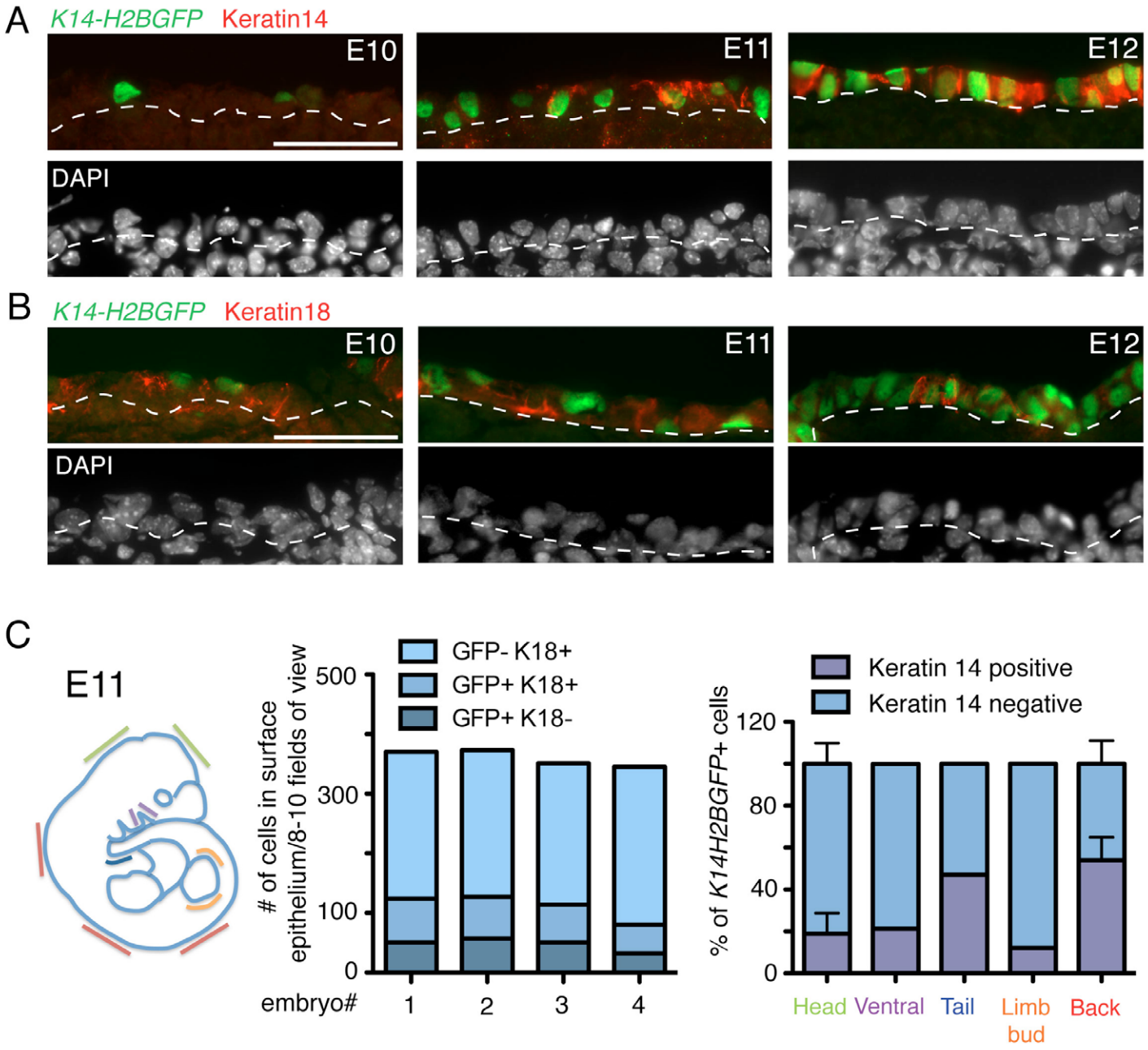

Fig. S2. Keratinocyte specification during embryonic development in *K14-H2BGFP* mice. (**A**) Immunofluorescence analysis of K14 expression during murine epidermal specification in a *K14*H2BGFP reporter mouse. Embryo sections immunostained with an antibody against keratin 14 (red) reveals that the keratin 14 promoter becomes activated (green) in the surface epithelium. (**B**) Immunofluorescence analysis of K18 expression in *K14-H2BGFP* mice during epidermal specification. Sections of *K14H2BGFP* embryos were immunostained with antibodies against keratin 18 (red). K18 expression within the surface epithelium is downregulated from E10 to E12 as keratinocytes are specified. (**C**) Quantification of the total number of surface epithelial cells that are $GFP^{+}K18^{+}$, $GFP^{+}K18^{-}$ or GFP-$K18^{+}$ and percentage of *K14H2BGFP*$^{+}$ cells that are $K14^{+}$ or $K14^{-}$ within the surface epithelium at E11 in several areas of the embryos. *n*=3-4 embryos for each bar. The dotted line indicates surface epithelium boundary. Scale bar: 50 µm.

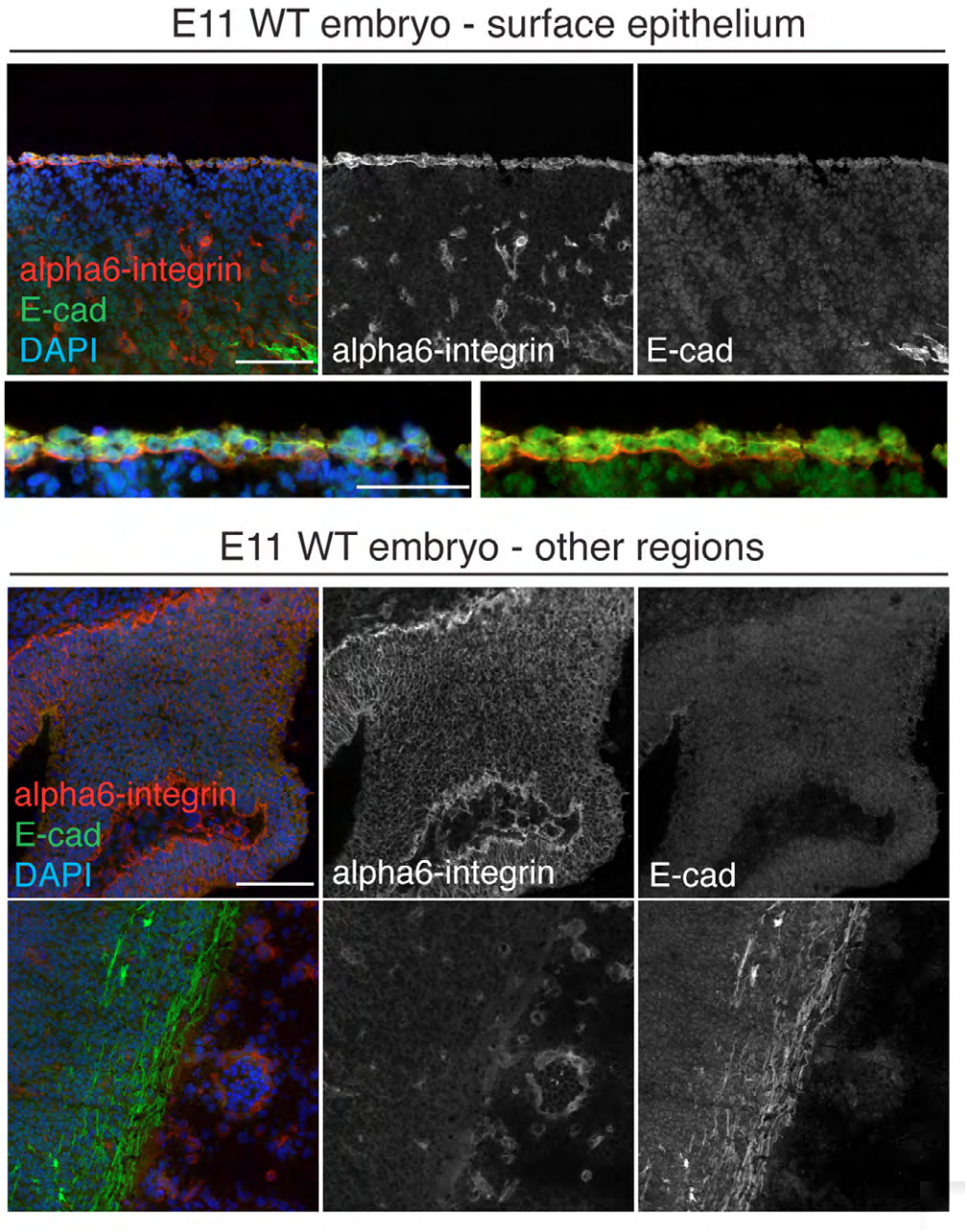

Fig. S3. Characterization of the embryonic murine skin populations isolated by cell sorting. At embryonic day 11 α6 integrin (red) and epidermal cadherin (E-cad, green) colocalize within the surface epithelium but do not colocalize in other areas of the embryo. Scale bar: 100 μm or 50 μm (insets).

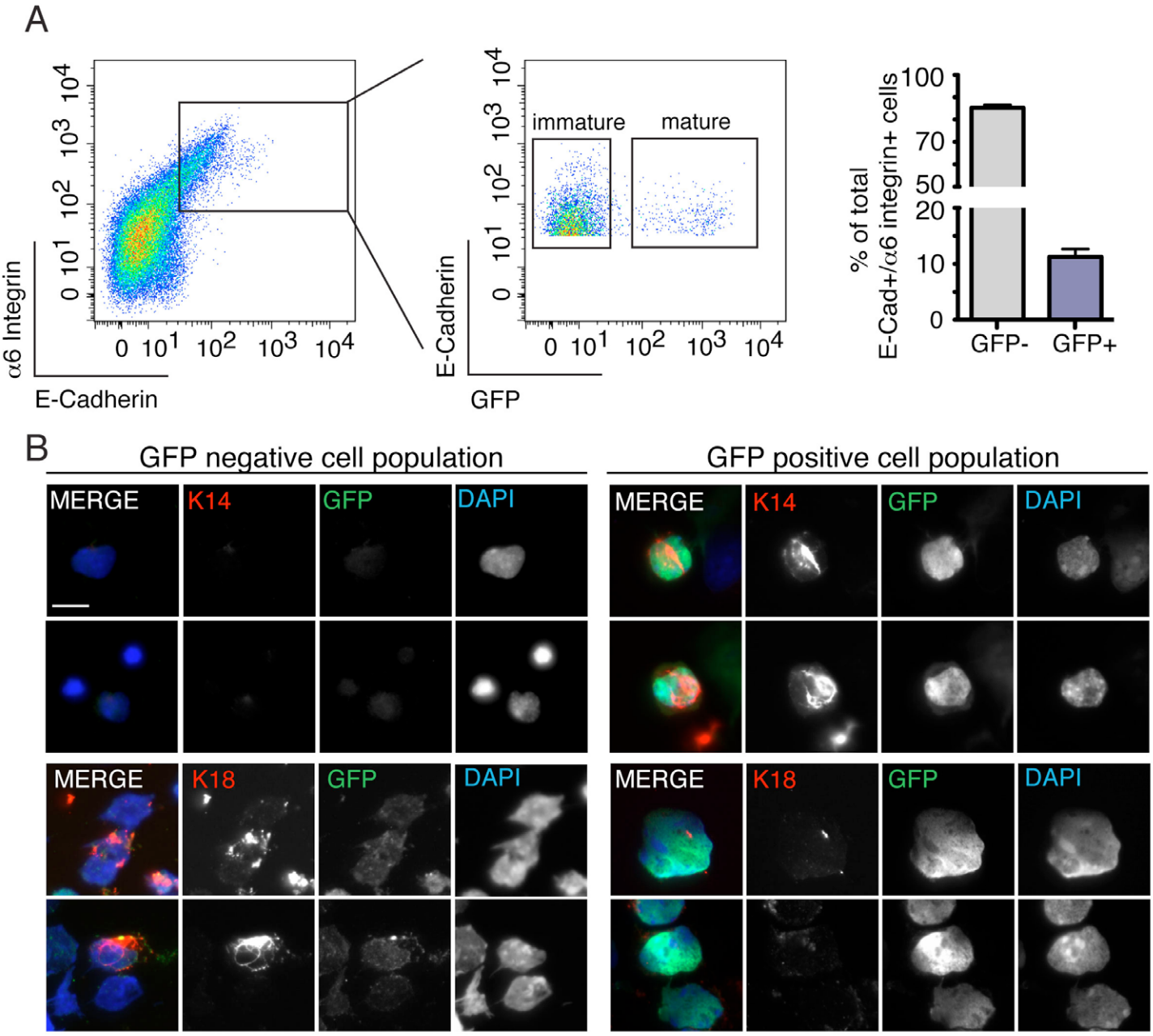

Fig. S4. Characterization of FACS-sorted E11 murine cell populations. (**A**) Dot plots and quantification of dissociated cells from E11 *K14-H2BGFP* embryos stained with antibodies against E-cadherin and α6 integrin (*n*=3 independent FACS-purified cell populations for each bar). (**B**) E11 E-cadherin^{+}, α6 integrin^{+}, GFP^{-} and E11 E-cadherin^{+}, α6 integrin^{+}, GFP^{+} cell populations isolated by cell sorting were characterized by immunofluorescence using antibodies for K14 and K18. Scale bar: 10 μm.

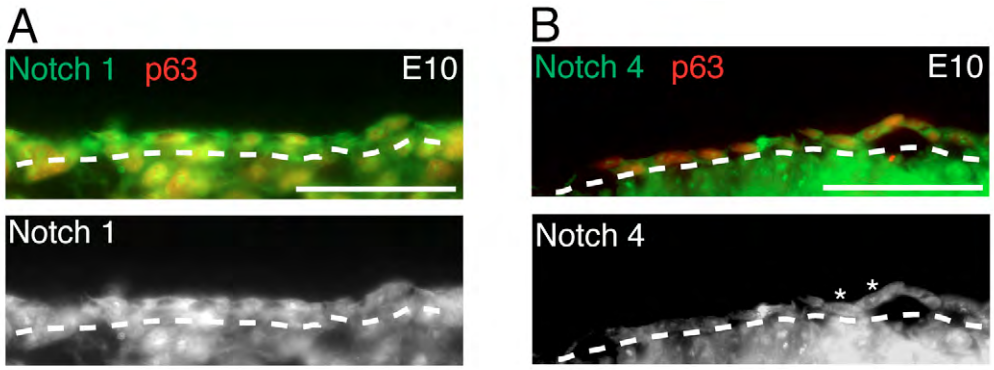

Fig. S5. Cellular localization of the Notch receptors Notch1 and Notch4 in E10 murine embryos. Immunofluorescence analysis of Notch1 (**A**) (green) and Notch4 (**B**) (green) and p63 (red) expression during murine skin development at E10. The dotted line indicates surface epithelium boundary. Scale bars: 50 μm.

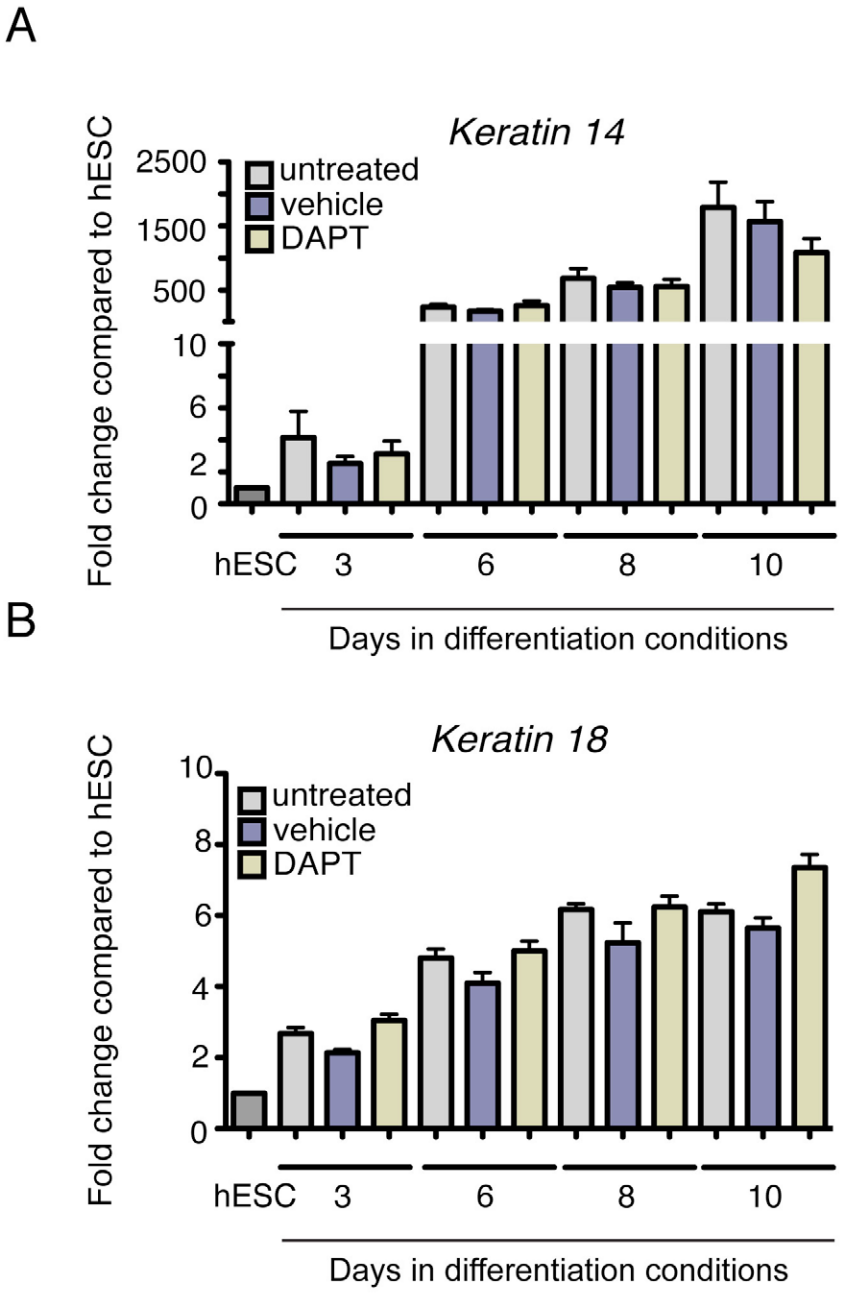

Fig. S6. Notch signaling inhibition does not affect mRNA levels of *K18* or *K14* in differentiated hESCs. Quantitative real-time PCR analysis does not reveal a significant change in mRNA levels for *K14* (**A**) and *K18* (**B**) when hESCs are treated with a Notch signaling inhibitor (DAPT) compared to untreated or vehicle-treated cells throughout the ectoderm differentiation protocol (n=9 independent sorting experiments for each graph bar for *K14* and n=6 independent sorting experiments for each graph bar for *K18*).

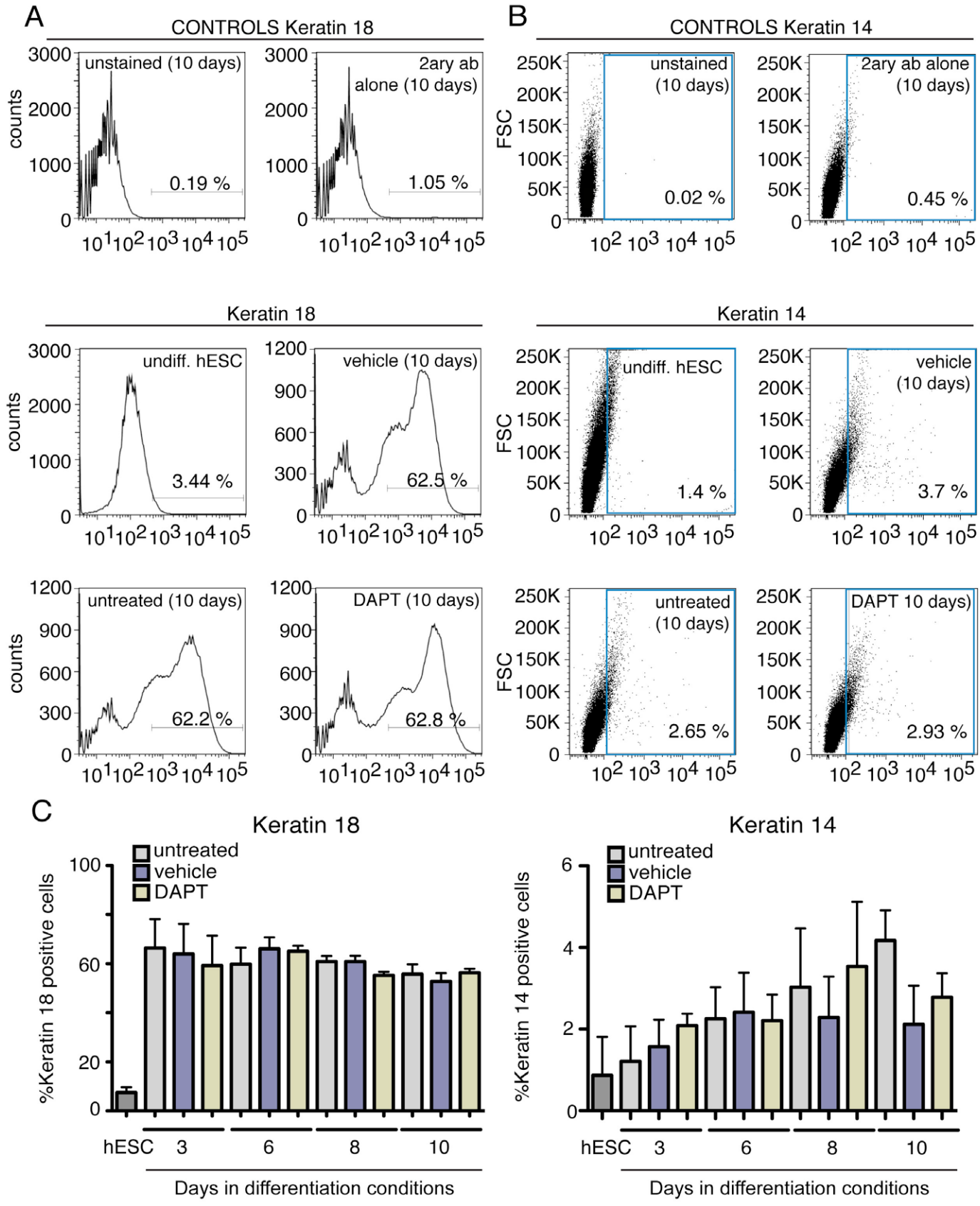

Fig. S7. Notch signaling inhibition does not affect the percentage of K14$^+$ and K18$^+$ cells after differentiation. (**A**) FACS analysis of hESCs reveals that upon differentiation there is a significant increase in the percentage of K18$^+$ cells, but this percentage is not affected when Notch signaling is inhibited by DAPT. (**B**) Similarly, there is a small increase in the levels of K14 at the end of the differentiation protocol, but this change is not affected by DAPT treatment throughout the differentiation protocol. Percentages of K18 or K14 are indicated on each plot. (**C**) Quantification of K14 and K18 FACS results shows that there are no significant changes in DAPT-treated cells when compared with untreated or vehicle treated cells throughout the entire differentiation protocol. All data are ± s.e.m. (*n*=3 independent differentiation experiments for each bar).

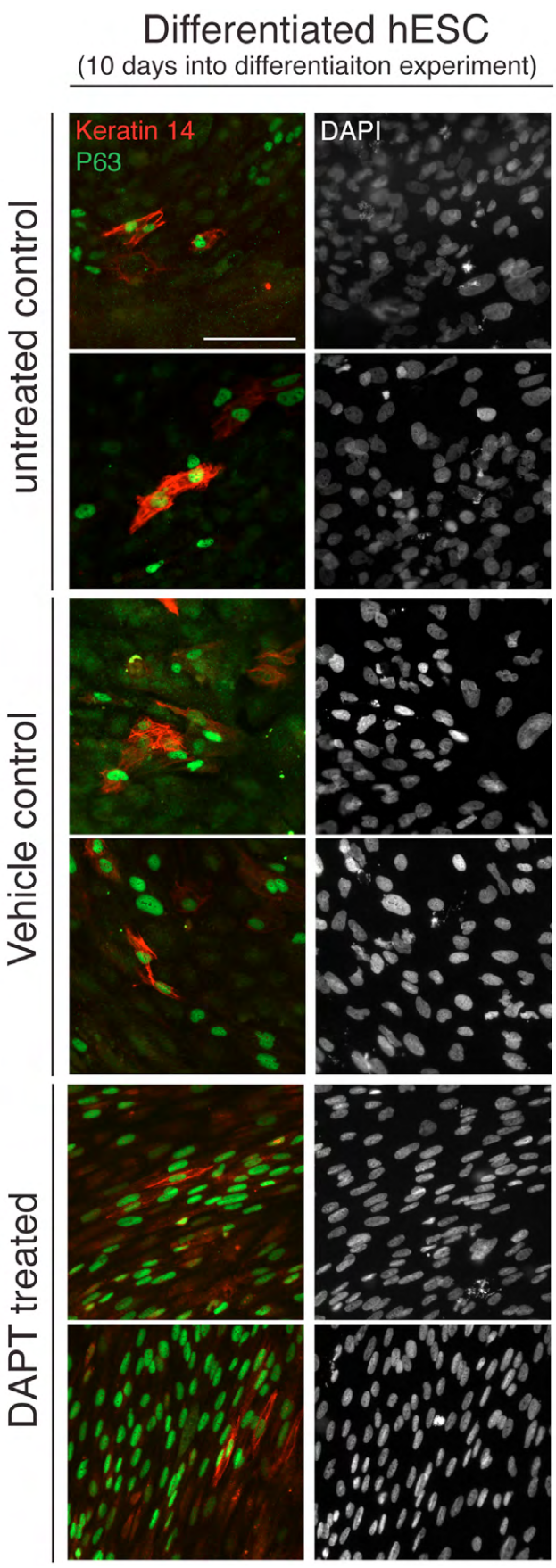

Fig. S8. Notch inhibition does not affect the numbers of Keratin 14 and P63 double positive cells after differentiation. Immunofluorescence analysis of differentiated hESCs using antibodies for K14 (red) and P63 (green) reveals that Notch signaling inhibition by DAPT does not affect K14/P63 double positive cells when compared to untreated or vehicle-treated cells. Scale bar: 100 μm.

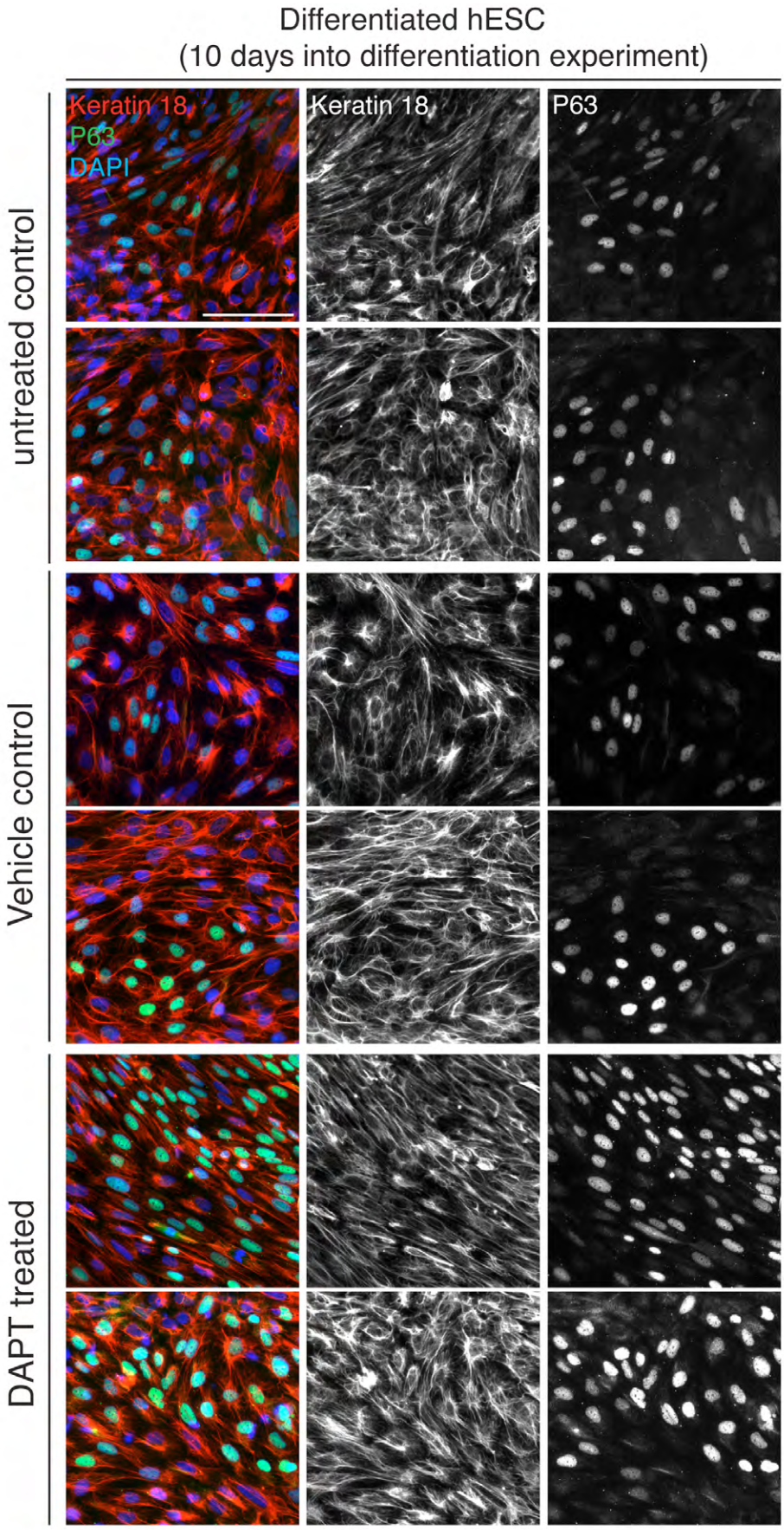

Fig. S9. P63 is expressed in K18^{+} ectoderm cells in the presence and absence of Notch signaling. Immunofluorescence analysis of differentiated hESCs using antibodies for keratin 18 (red) and P63 (green) reveals that P63^{+} keratinocyte progenitors express keratin 18 and that this expression pattern is not affected when cells are treated with the Notch signaling inhibitor DAPT throughout the differentiation protocol. Scale bar: 100 μm.

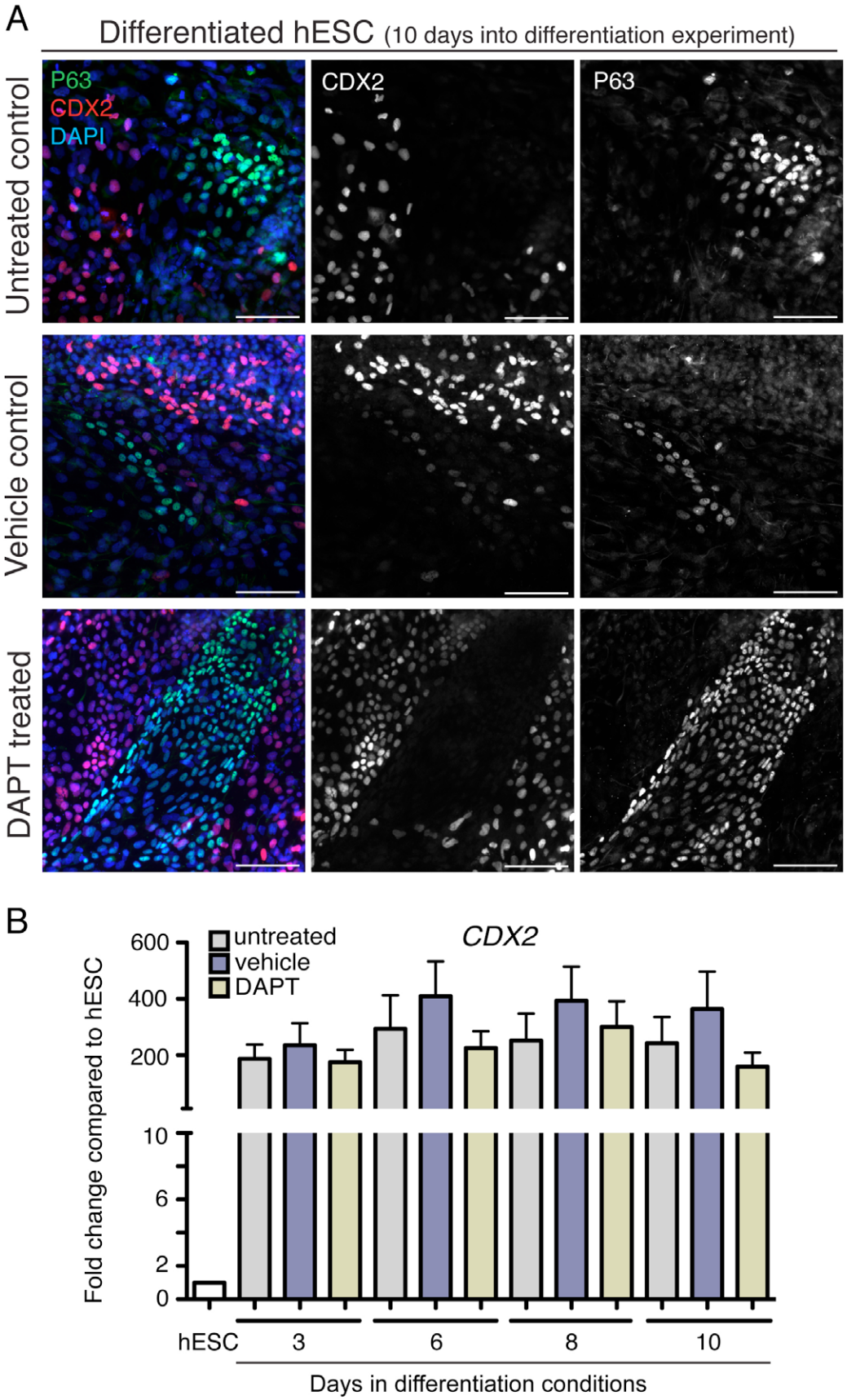

Fig. S10. Notch signaling inhibition does not alter trophoblast formation during hESC differentiation. (**A**) Treatment of hESCs throughout the entire differentiation protocol with the γ-secretase inhibitor DAPT leads to an increase in the numbers of P63-positive cells (green) that are CDX2 (red) negative. (**B**) Quantitative real-time PCR reveals that the global levels of *Cdx2* mRNA do not significantly change when Notch signaling is inhibited by DAPT compared to untreated or vehicle-treated control experiments. All data are ± s.e.m. (*n*=9 independent differentiation experiments for each graph bar). Scale bar: 100 μm.

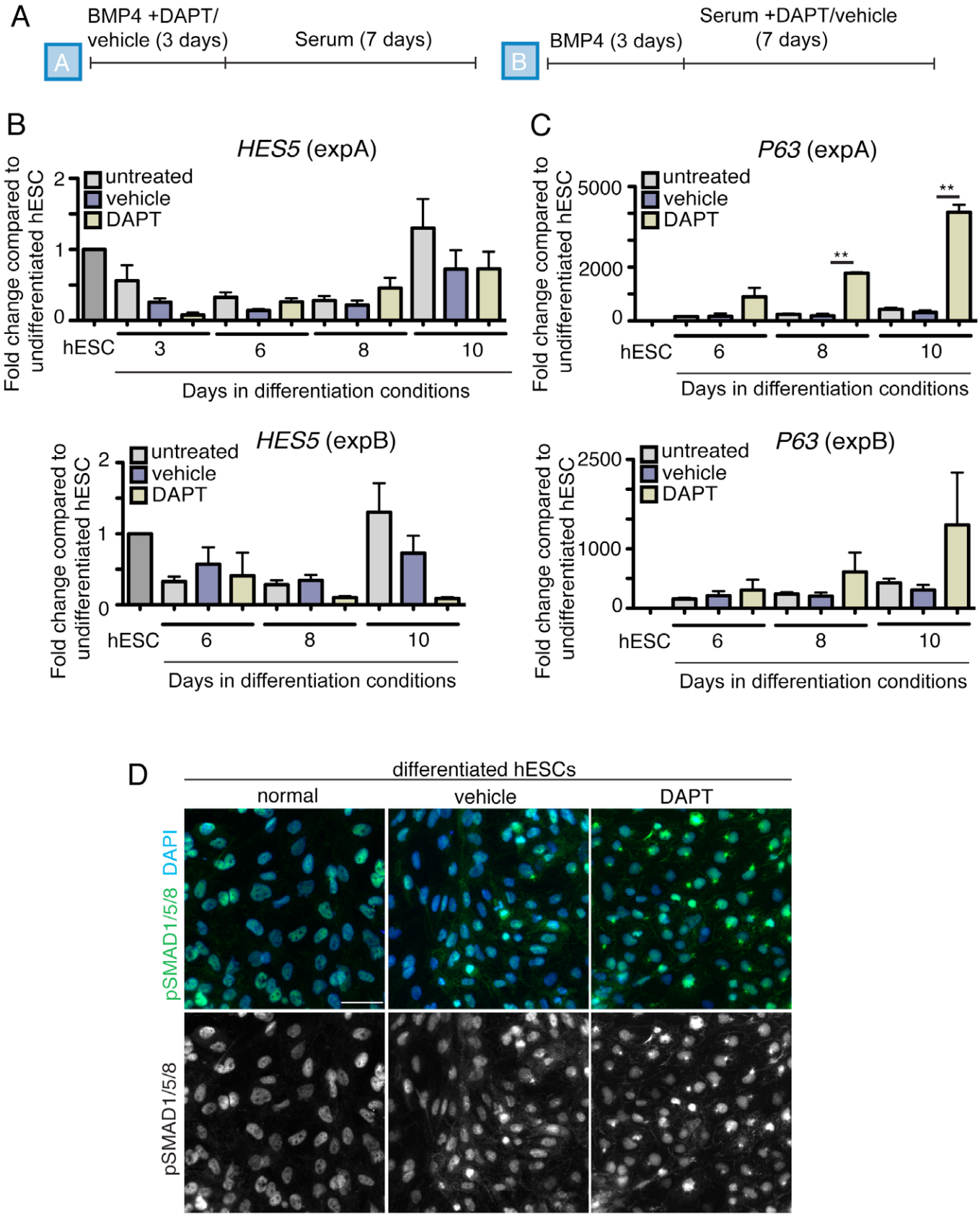

Fig. S11. Inhibition of Notch signaling during BMP treatment is required to increase P63 expression in hESCs. (**A**) hESCs were treated with vehicle or DAPT either during the BMP4 treatment (first 3 days) or after BMP4 treatment (days 4-10). (**B**,**C**) Quantitative real-time PCR analysis of mRNA levels of *HES5* and *P63* shows that inhibition of Notch signaling during BMP4 incubation was sufficient to induce an increase in the levels of P63 mRNA. All data are ± s.e.m. (**0.001<*P*<0.01) (*n*=3 independent differentiation experiments for each bar). (**D**) Immunofluorescence analysis of pSMAD1/5/8 (green) expression in ectoderm specified hESCs reveals that inactivation of Notch signaling with DAPT does not affect the levels of pSMAD1/5/8. Scale bars: 50 µm.

Table S1. Mouse (*Mus musculus*) primers used for quantitative real-time PCR analysis

Gene	Fw primer	Rev primer
keratin 18	GACGCTGAGACCACACT	TCCATCTGTGCCTTGTAT
keratin 14	AGGGAGAGGACGCCCACCTT	CCTTGGTGCGGATCTGGCGG
Trp63	ACGCCCCGCCTCTTTGCAAAT	TGAGCTGGGGTTTCTATGAAACGCT
Eya4	ACAGCTGTACCCCTCCAAGCCC	TAGACGGCCGGCTGCTGCAT
Gata2	CCGCCTCCAGCTTCACCCCTA	TGCACAGGTAGTGGCCCGTG
Irf8	GCAACGCGGTGGTGTGCAAG	ACAGCTGCTCTACCTGCACCAGA
Gbx2	GCAAGTTCGCTCCACAGCCAC	AGCTCTCCTCCTTGCCCTTCGG
Six1	GGCCAAGGAAAGGGAGAACACCG	TGAGCTGGACATGAGCGGCTTG
Notch1	GGCTGCACAGAAGCGAGGCAT	CTGCCCGTGTAGCCTGCCTG
Notch2	TTCGTGTCCCCCAGGCACCC	AATCCGGTCCACGCACTGGC
Notch3	GCACCCCCTTGTCTGGATGGA	GTGCCCGCCACCACTGAACTC
Notch4	ACCTGTGTGCCTCAGCCCAGT	GGGCTGGGACTGACAAGCGTC
Jag1	TGGACTGGCCCCACGTGTTC	GGGCGGGCACACACACTTGAA
Jag2	ACCCGGGCCTCGTCGTCAT	TGCAGGCTCTTCCAGCGGTC
Dll1	CGGGCCAGGGGAGCTACACA	AGCTGTCCTCAAGGTCCGTGC
Dll3	TGCCCTTCCGCGATGCTTGG	CTCCCATGTGCCTGTGCGCT
Dll4	CAGCATCCCCTGGCAGTGTGC	GCTGGCACACTTGCTGAGTCCC
Dlk1	CCCCCTGCGCCAACAATGGA	CCGTGCTGGCAGGGAGAACCAT
Dlk2	CCTGCCAGAGCGGATGACTGC	CTCACAGTGCAGCCCCTCCCA
Dner	GCCCAGCTGGTGGACTTCTGC	GGCCATGGTAACCTGGATCGC
Hey1	GCGCCGACGAGACCGAATCAA	CAGGGCGTGCGCGTCAAAAT
Hes5	GCTCCGCTCGCTAATCGCCT	CCGGCTTCCGCAGTCGGTTTTT

Table S2. Human (*Homo sapiens*) primers used for quantitative real-time PCR analysis

Gene	Fw primer	Rev primer
keratin 18	TGAGACGTACAGTCCAGTCCTT	GCTCCATCTGTAGGGCGTAG
keratin 14	TCAGCATGAAAGCATCCCTGGAGAA	ATTTGGCGGCTGGAGGAGGTCA
TRP63	AGCCAGAAGAAAGGACAGCAGCATT	CTGTGCGGGCCTGGGTAGTC
OCT4	CCCCTGGTGCCGTGAAGCTG	CCCCAGGGTGAGCCCCACAT
CDX2	CGGCGGAACCTGTGCGAGT	TGGCGGCTAGCTCGGCTTT
SOX1	TCTATGCTCCAGGCCCTCTCCTCG	GGACCACACCATGAAGGCGTTCA
FOXA2	GAGCAGCAGCGGGCGAGTTA	CCCAGGCCGGCGTTCATGTT
NOTCH1	CTACGTGTGCACCTGCCGGG	CGTTTCTGCAGGGGCTGGGG
NOTCH2	GCACTCGGGGCCTACTCTGTGAAGA	AGGGGTTGGAGAGGCACTCGT
NOTCH3	GTGGACGAGTGTGCTGGCCC	CGGCGAAACCAGGGAGGCAG
NOTCH4	TCCCCAGCTCTCCCTCTCCATTG	CAGAAGTCCCGAAGCTGGCACT
JAG1	TGCGAGCCAAGGTGTGTGGG	CGTGGACCCTGAGCCGAAGC
JAG2	ATCAACGTCAACGACTGTCGCGGG	TATAGCAGCGAGCGCCGTTCC
DLL1	GCAGCCCTGGCAGTGCAACT	CGAGATCCGTGCAGCTCCCT
DLL3	ATCTACGCTCGGGAGGCCTGAC	AGACTGGGCACCACCGAGCAA
DLL4	ACCTTGAGCTGCGCCGACTC	CACTGTCCCCCGTTGGCACA
DLK1	ACCTGCGTGAGCCTGGACGA	GCAGGGGGAGCCGTTGATCAC
DLK2	GAGGTGTCCACGCGTCCGGC	CGCTCACAGTGCAGCCCCTC
DNER	GGGATCTCCGGCGCCAACTG	AAGCTGTCGGGGTGCCATGG
HES1	ATGACGGCTGCGCTGAGCAC	TAACGCCCTCGCACGTGGAC
HES5	CCGGTGGTGGAGAAGATG	GACAGCCATCTCCAGGATGT
HEY1	TGAGCTGAGAAGGCTGGTACCCA	TGCGCGTCAAAGTAACCTTTCCC